

High Purity Hydrogen From Coal in a Single Step

Kanchan Mondal¹, Lubor Stonawski¹, Krzysztof Piotrowski², Tomasz Szymanski¹, Tomasz Wiltowski^{1,2}

¹Department of Mechanical Engineering and Energy Resources

²Coal Research Center,

Southern Illinois University, Carbondale, IL 62901

ABSTRACT

The production of high purity hydrogen from steam gasification of coal has been investigated. The separation of carbon monoxide from hydrogen in the gasification products is achieved by carbon monoxide oxidation to carbon dioxide followed by uptake of the carbon dioxide by a suitable removal agent. This uptake of carbon dioxide increases the water gas shift reaction and enhances the yield and purity of hydrogen. In addition to water gas shift reaction, the oxidation is enhanced by the use of a solid oxygen transfer agent (hematite) in the hydrogen enrichment pass. Subsequently, the reduced oxygen transfer agent is reoxidized (and thus regenerated) in the presence of air and the heat liberated via the exothermic reaction is utilized to regenerate carbon dioxide removal agent. In this study, the effect of process variables on coal gasification and hydrogen enrichment have been evaluated. Thermogravimetric analysis (TGA) were conducted to understand the mechanism of iron oxide reduction in syngas atmosphere and the uptake of CO₂ by lime. TGA experiments were also conducted to evaluate the long term effects of cycling of CaO and Fe₂O₃. Fixed bed gasification studies using coal and coal-hematite and coal-CaO mixtures were conducted to evaluate the kinetics of gasification and separation effectiveness of the process. Finally, a bench scale fluidized bed reactor was employed to study the efficacy of the simultaneous gasification-hydrogen enrichment process. The reactions were conducted in the temperature range of 670°C -900°C at atmospheric pressures. The results from the fundamental studies, the fixed bed reactor studies and the fluidized bed reactor studies are presented.

INTRODUCTION

Hydrogen is an important raw material; in the chemical industries such as in the manufacture of ammonia, methanol, etc.. The possibility of hydrogen as a future energy source in heating, electric power and transportation sectors will cause a huge increase in the hydrogen demand. Conversion of natural gas and other light hydrocarbons is currently the major process for hydrogen production. Coal and petroleum coke may serve as raw materials for hydrogen production in the future.

The first step of forming hydrogen from coal is gasification (Cox, 2004, Ruby et al, 2004, De Biasi, 2003, Pierce, 2003, Vambuka, 1999, Hauserman, 1994, Ageeva and Chernenkov, 1993) followed by water gas shift reaction (Qi and F-Stephanopolous, 2004, Zhao and Gorte, 2004, Hillaire, et al, 2001). Reforming reactions are highly endothermic and thermodynamically favored by high temperature and low pressure. On the other hand, the water gas shift reaction is favored by low

temperature and is not pressure dependent. Due to the overall endothermic nature, gasification is generally conducted at high temperatures. Thermochemical conversion of carbonaceous raw materials to high yield hydrogen via the use of catalysts is gaining attention from several researchers (Minowa and Inoue, 1999). Ca based catalysts are known to promote steam gasification at relatively moderate reaction conditions. Thermogravimetric studies and high temperature x-ray diffraction analysis to investigate the catalytic effects of C-based compounds showed that the addition of calcium compounds decreased the reaction temperature and increased the gasification rates (Ohtsuka and Tomita, 1986). In their investigations, Balasubramanian et al (1999) found that the addition of NiO/Al₂O₃ and CaO successfully achieved near equilibrium conditions for reforming of methane, water gas shift and the separation of CO₂ simultaneously in a single reactor at 50 °C.

Finally, separation of the carbon dioxide and hydrogen (Lin et al 2004, Lin et al, 2002, Lin et al, 2001, Rukowski et al 2002, Egan et al 1991, Egan et al, 1992) needs to be achieved. Separation of H₂ from the coal gasification products supports existing H₂ markets (such as refineries and power production) and makes hydrogen economy a distinct possibility. The sequestration-ready aspect of H₂/CO₂ separation will be of consequence in power applications in the future. It must also be noted that carbon monoxide in the hydrogen gas stream acts as a poison to the catalysts used in electrodes employed in fuel cells necessitating its removal. Existing technologies utilize the water gas shift reaction for the conversion of CO to CO₂. The carbon dioxide is then separated from hydrogen by absorption (Selexol, Rectisol, A-MDEA, Purisol, Sulfinol, UCARSOL, amines), adsorption (molecular sieves, activated carbon), cryogenic separation, and membrane separation (polymer, metal, facilitated transport membrane, molecular sieves), all of which are costly alternatives. In addition, a methanation step may be required to follow the amine scrubbing step to reduce the CO_x to trace levels. In the pressure swing adsorption technology, no further purification is required but at the cost of hydrogen yield.

The CO₂ generated, a greenhouse gas with a potential to contribute to global warming, is generally released to the atmosphere. With stringent environmental regulation already in place and the requirement for zero emissions in the future, it is important to develop means to capture/sequester CO₂ from the process. In the current context, in situ capture of CO₂ not only provides a chance to sequester the greenhouse gas, but also increases the conversion to and the purity of the hydrogen stream by removing the thermodynamic limitations at a given condition. Given that a CO₂ acceptor is available, near zero CO content in the outlet gas may also be achieved. The first attempt of using CaO in a “CO₂ acceptor process” was conducted by Curran et al (1966) and McCoy et al (1976). In these studies only 50 % of CO and CO₂ was immobilized in the solids. However, later studies in a micro-autoclave (Lin et al, 1999, 2000) product gases consisting of primarily H₂ and CH₄ were obtained. Upto 84 % purity hydrogen stream was reported by Lin et al (2002) in a pressurized bed reactor. The pressurized bed reactor provided higher rates of CH₄ decomposition resulting in the higher H₂ contents. A new method, Hydrogen Production by Reactions Integrated Gasification (HyPr-Ring), that combines the gas production and separation reactions in one reactor was suggested by Lin et al (1999). In this process the energy required for the endothermic reforming reactions were provided by the heat of CO₂ absorption. Wang and Takarada (Wang and Takarada, 2001) reported that complete fixation of CO₂ with Ca(OH)₂ could be achieved for a Ca/C molar ratio of 0.6 (stoichiometry dictates the ratio to be 1) along with significantly enhanced decomposition of tar and char. Kuramoto et al (Kuramoto et al, 2003) also investigated C-CaO-H₂O system, using subcritical steam (50 – 150 °C). They reported an increase in the CH₄ content due to the addition of Ca(OH)₂, along with the yields of hydrogen.

The overall conversion rates of CO to CO₂ may be enhanced by including an oxygen donor in the reaction zone. An added advantage of this process is that steam reforming rates of methane and

other hydrocarbons released during coal pyrolysis will also be increased. Iron oxide is known to show WGS activity at high temperatures. Thermodynamic analysis also shows that the FeO-Fe₂O₃ transition has ideal enthalpy characteristics for the WGS reaction necessary to convert syngas to hydrogen. However, iron oxide is found to oxidize hydrogen at a much faster rate (nearly 3-4 times) as compared to CO. This would result in a reduction in the yield of hydrogen. The reduction of iron oxide and various ores containing iron oxide have been studied in the past. Various controlling mechanisms have been suggested in their research. Shimokawabe (1979) suggested a random nucleation mechanism for the reduction of hematite (Fe₂O₃) while phase boundary mechanism was evoked in Sastri *et al.*'s research (1982). In 2001, Tiernan *et al.* (2001) concluded that reduction of hematite to magnetite (Fe₃O₄) was via phase boundary while that of magnetite to free iron was via random nucleation. Ishii *et al.* (1986) found that the reduction of Fe₂O₃ was 10 times faster in H₂ atmosphere as compared to CO atmosphere. In 1997, Moon and Rhea (1997) estimated that the reaction rate for Fe₂O₃ reduction with CO was 2-3 time lower than that with H₂. They estimated the value of the apparent activation energy for iron oxide reduction to be 14.6 kJ/mol in a carbon monoxide atmosphere. In a later work (Moon et al, 1998), they estimated the activation energy for the reduction reaction in CO to be 19.8 kJ/ mol in pure CO stream, the value of which increased with reducing CO partial pressure in a CO-H₂ gas stream. The value of the activation energy was found to be 42.1 kJ/mol in a 100% hydrogen atmosphere. Thus, the effect of Fe₂O₃ on simultaneous coal gasification and H₂ separation needs to be investigated. Nikanorova and Antonova (1991) reported an increase in hydrogen yield by 1.5 times due to the addition of iron-oxide to lignite prior to gasification with a final purity of 60 %. Zhu and Wang (2003) evaluated the effect of iron oxide on atmospheric pressure mild gasification of shenmu bituminous coal, over the temperature range 450°C-750°C in a fluidized bed. Their results of experiments indicated that the iron oxide significantly increased hydrogen yield while decreasing the CO yield.

The non volatile components present in tars present several engineering problems along with increasing the need for a hot gas purification step in gasification processes. Among the alternatives, catalytic steam gasification appears to be attractive. Studies (Garcia et al , 1999) have shown that limestone to be effective catalysts for gasification of model compounds found in tars. Several researchers (Hesp and Waters, 1970, Brage et al, 1996)] have shown similar effects with real tars. In addition, Li et al (2001) reported that Fe₂O₃-CaO mixtures were efficient in sulfur removal in IGCC processes through multiple desulfurization-regeneration cycles. Researchers (Otsuka et al, 2001, Prilepskaya, 1991) have shown the effect of iron oxide on the degradation of coal and other hydrocarbons.

The focus of this research is also to investigate the reaction conditions that result in the oxidation of carbon monoxide to carbon dioxide. Carbon dioxide would then be removed by lime. TGA studies were conducted to evaluate the effect of temperature and gas composition on the reactions, along with parametric (steam, temperature, Fe₂O₃ loading, CaO loading) evaluation on hydrogen yield and purity in a fluidized bed reactor. Finally, additional experiments were conducted in a fixed bed reactor to verify and compare the results obtained in a fixed bed reactor. The Gibbs free energy data show that the reduction of hematite to wustite is favored at high temperatures. However, the capture of carbon dioxide via lime is generally favored at temperatures less than 900 °C. Nonetheless, the temperature window of 725 – 900 °C affords thermodynamically favorable reaction conditions for both the oxidation of CO to CO₂ using iron oxide and the subsequent sequestration of CO₂ by lime. In addition, carbon monoxide disintegration and iron carbide formation is not thermodynamically favored at temperatures greater than 725 °C. Hence, in this investigation, the temperature range of 725 – 900 °C was studied for the oxidation of CO.

PROCESS CONCEPT

The basic idea of the process lies in the simultaneous use of a) an oxygen transfer compound (OTC) to enhance the conversion rates of carbon monoxide to carbon dioxide along with the water gas shift reaction present in syngas and b) capture of CO₂ using an appropriate carbon dioxide removal material (CDRM) leading to the production of high purity hydrogen stream. The net of these reactions is exothermic and so additional CO₂ and H₂ is produced by methane reforming. Subsequently the reduced OTC is oxidized (and thus regenerated) in the presence of air/oxygen and the heat liberated via the exothermic reaction is utilized to regenerate CDRM. In this paper we investigate iron oxide as the OTC and CaO as the CDRM. Figure 1 presents a schematic of the overall process. Thus, the products of this system would result into three separate streams of a) high purity hydrogen for use in fuel cells; b) sequestration ready CO₂; and c) high temperature (pressure) oxygen depleted air for use in gas turbines.

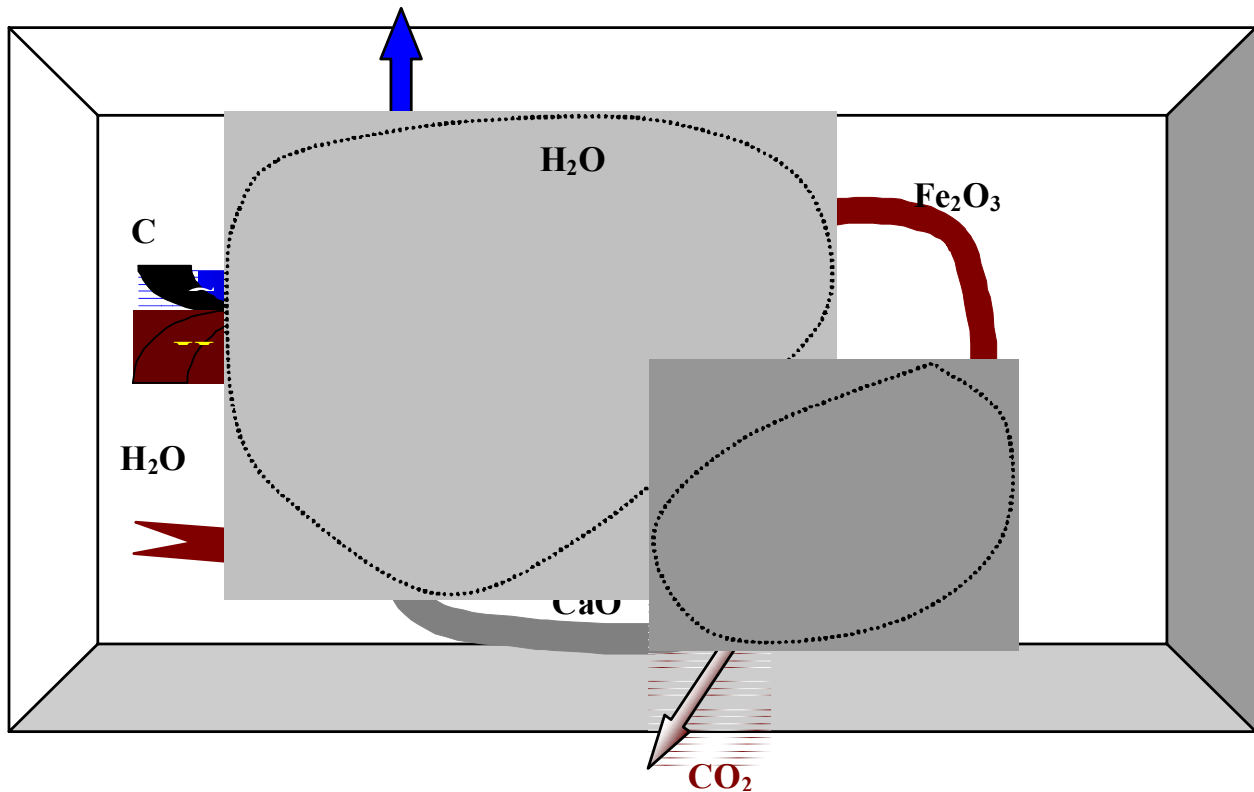
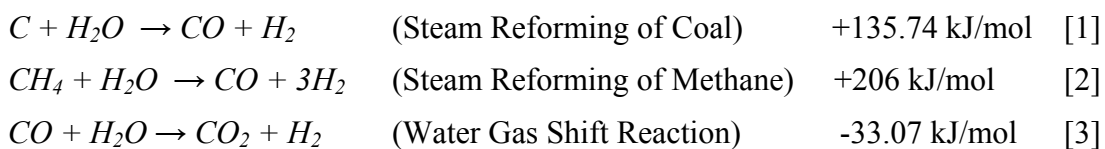


Figure 1 Schematic of the Overall Process

The following are the reactions expected to take place in the reactor. The heats of reaction are calculated for 800 °C.



$2 CO \rightarrow CO_2 + C$	(Boudouard Reaction)	-169.44 kJ/mol	[4]
$CO + Fe_2O_3 \rightarrow 2 FeO + CO_2$	(CO oxidation)	-4.75 kJ/mol	[5]
$CaO + CO_2 \rightarrow CaCO_3$	(CaO Carbonation)	-168.69 kJ/mol	[6]
$CaO + H_2O \rightarrow Ca(OH)_2$	(CaO hydration)	-94.05 kJ/mol	[7]
$Ca(OH)_2 + CO_2 \rightarrow CaCO_3 + H_2O$		-74.67 kJ/mol	[8]
$CH_4 + CO_2 \rightarrow CO + 3H_2$	(Dry Reforming of Methane)	+260.76 kJ/mol	[9]
$C + 2 H_2 \rightarrow CH_4$	(Methanation)		[10]
$H_2 + Fe_2O_3 \rightarrow 2 FeO + H_2O$	(+28.97 kJ/mol	[11]
$C + Fe_2O_3 \rightarrow CO + 2FeO$	(Solid Catalyzed C oxidation)	+9.39 kJ/mol	[12]

Oxide Regeneration Stage:

$FeO + O_2 \rightarrow Fe_2O_3$		-281.4 kJ/mol	[13]
$CaCO_3 \rightarrow CaO + CO_2$		+167.6 kJ/mol	[14]

THERMODYNAMIC ANALYSIS

Equilibrium gas compositions were calculated for four reaction systems, namely a) C-H₂O, b) C-CaO-H₂O, c) C-Fe₂O₃-H₂O, and d) C-CaO-Fe₂O₃-H₂O at 1 bar under different temperature conditions. For each of the reaction systems the ratio of C:H₂O was set at 0.5. The ratio of C:CaO and C: FeO were set at 1 for relevant cases. Figure 2 shows the equilibrium composition of the product gases in each reaction system. It is seen that simple steam gasification produces a stream with a maximum hydrogen content of 57 %. The CO₂ content is observed to decrease while that of CO increases with temperature due to the exothermic nature of the water gas shift reaction. The methane content decreases with temperature due to the increased proportion of methane reformation and decreased levels of methanation. Ideally, the three moles of gas should be produced per mole of C with a hydrogen purity of 66.67 %. With simple steam gasification, a maximum of 1.36 moles of gas/mol of C was produced in the range of 700 – 775 °C. On adding CaO, the maximum total moles of dry gas in the exit stream were 1.46 per mole of C. However, one must consider that approximately 1 mole of CO₂ would be removed from the gaseous stream by CaO per mole of C gasified. The use of CaO showed the potential of obtaining a gaseous stream with hydrogen content of more than 90 %. With an increase in temperature (greater than 650 °C) the hydrogen concentration decreases while that of CO and CO₂ increases. The use of Fe₂O₃ during C gasification decreased the hydrogen content in the dry gas and the yield of moisture free gases, primarily due to the oxidation of H₂ to water. The amount of CO₂ produced is also higher than simple steam gasification due to the CO oxidation by Fe₂O₃. It is also observed from the figure that the methane content in the gaseous mixture is lower than both the reaction systems described earlier. This is a result of both higher degree of dry reforming of methane by CO₂ as well as partial oxidation by Fe₂O₃. The use of both CaO and Fe₂O₃ during steam gasification of C provided a high yield of equilibrium dry gas mixture with the highest hydrogen content. In the temperature range evaluated the hydrogen concentration content varied between 98.3 to 99.4 %. The gas yield ranged from 1.15 to 1.7 moles/mole of C.

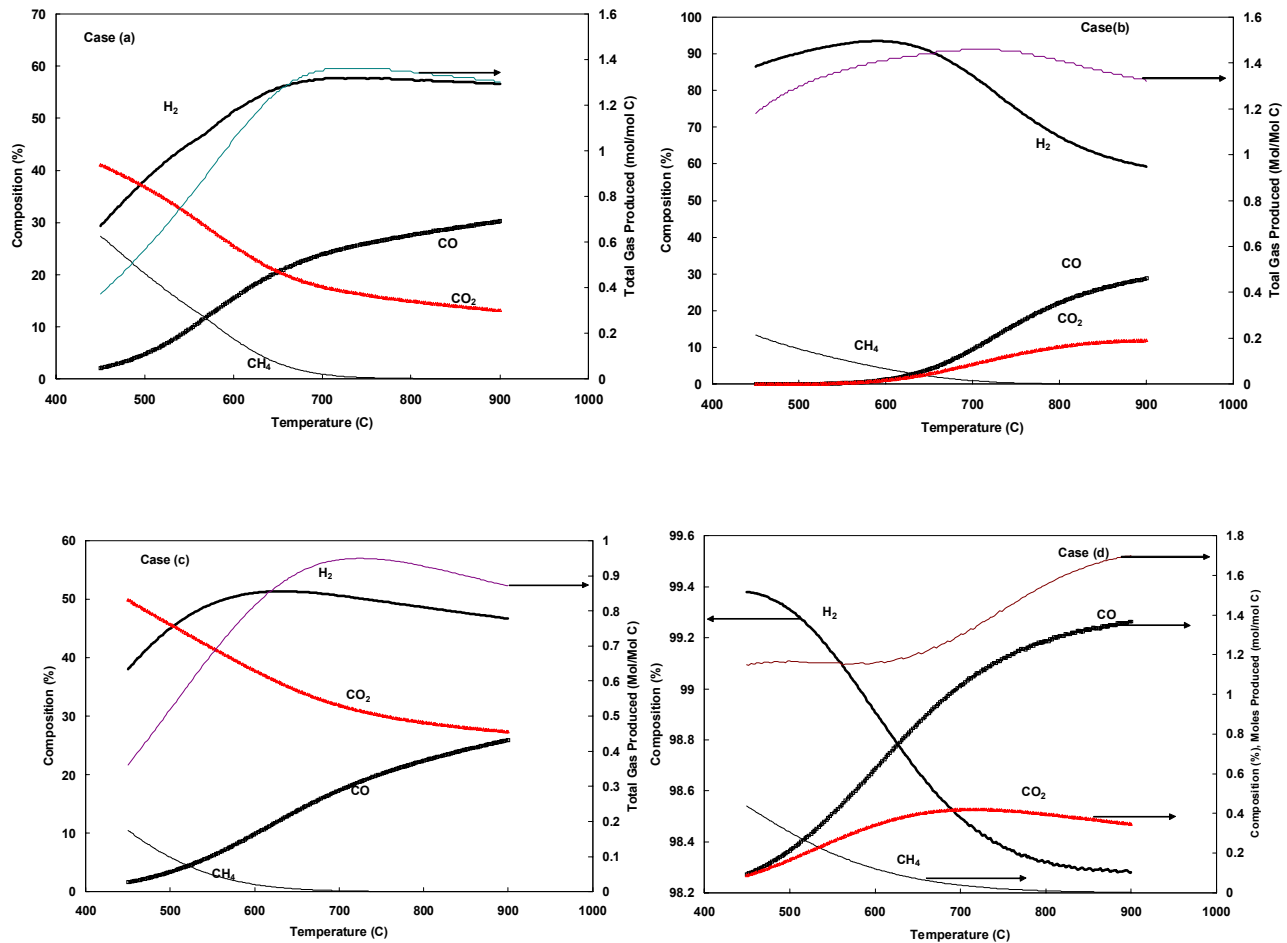


Figure 2: Equilibrium Dry Gas Compositions for reaction systems: a) C-H₂O, b) C-CaO-H₂O, c) C-Fe₂O₃-H₂O, and d) C-CaO-Fe₂O₃-H₂O

EXPERIMENTAL

Materials:

Pulverized Utah coal 355-420 was used for this study. The combustibles content was 73.30 %, while the ash and moisture contents were 7.85 and 8.68 % respectively. The size ranges of CaO (from Mississippi Lime Company, MO), iron oxide (Fisher Scientific, Chicago, IL) and silica sand used were 75-106 μm.

Thermogravimetric Analysis

All experiments were performed using the *Perkin-Elmer TGA-7* thermogravimetric analyzer with *TAC 7/DX* control box upgrade driven by *Pyris* software. Samples of Fe₂O₃ /CaO were preheated (heating rate 10⁰/min) under N₂ atmosphere to the desired temperature. While studying the iron

reduction characteristics, the samples were isothermally heated under reducing atmosphere (mixture composition: CO – 5.7%, H₂ – 4.3%, N₂ – 90%) till reduction process was finished. Experiments were terminated immediately when sample weight started to increase as a consequence of Boudouard reaction $2\text{CO} \rightarrow \text{C} + \text{CO}_2$ resulting in carbon deposition and/or FeC complex compounds formation. Air was used during iron oxide regeneration studies. Gas flow rate cross sample was 30 ml/min, the gases were dried before use in molecular sieve moisture trap (*Hydro-Purge II, Alltech*). For the calcinations carbonation studies of CaCO₃/CaO, the gases used were nitrogen and CO₂, respectively. Fe₂O₃/CaO samples initial weights in all cases were approx. 12 mg.

Fixed Bed Experiments

Pulverized coal sample with initial weight of 0.2g, as received, was placed so that it constituted as a “packed bed” in a quartz glass tube reactor of inner diameter of 1 cm. CaO/Fe₂O₃ was also packed inside the quartz tube. The schematic of the reaction system is shown in Figure 3. Nitrogen at 30 psig was used as a carrier gas. Samples were heated to the desired temperature and steam was introduced. A “cold” trap was located before the sampling outlet to condense all tar components. The progress of the reactions was followed by consequent sampling of the product gases for further gas chromatography analysis (Gow-Mac series 600).

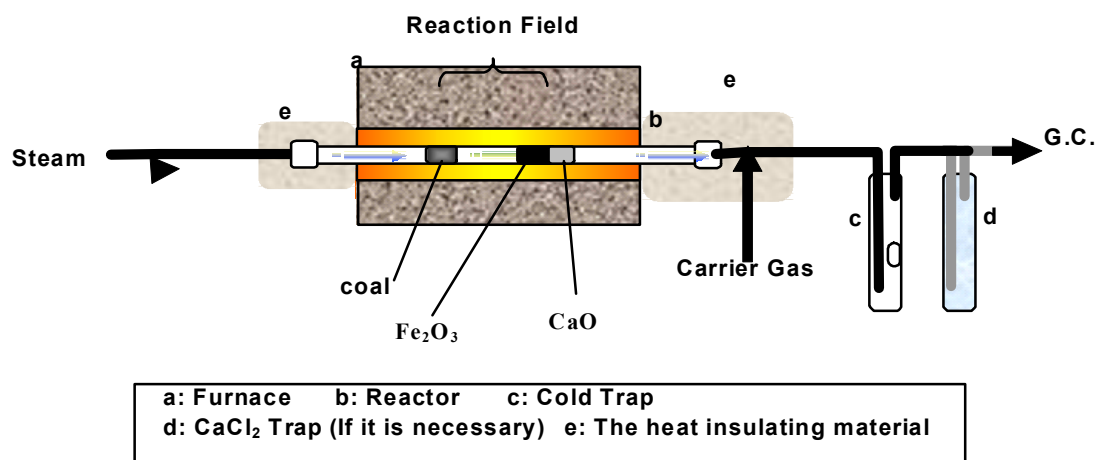


Figure 3 Schematic of the Fixed Bed Reactor

Fluid Bed Experiments

The oxides and sand mixture to be fluidized were inserted into the reactor (Figure 4) and the reactor was heated up to the desired temperature in the nitrogen flow at atmospheric pressure. Furnace temperature was set to the predetermined temperature. Measurement of temperature profile inside the reactor revealed inner temperature approximately 1 inch above bed was 810⁰C. After required thermal conditions had been stabilized, steam was introduced into the reactor. Flow of generated steam and nitrogen was adjusted in order to obtain the total gas mixture linear flow rate equal to 15 times the minimum fluidization velocity. Steam content in the reactor atmosphere was maintained at the desired level. Pulverized coal samples were injected into reactor using the solids delivery system driven by nitrogen. Immediately after coal injection, the outlet gas samples were collected at one-minute interval and the outlet volumetric flow rate was recorded, for duration of 30 minutes. Collected gas samples were analyzed using gas chromatography (GOW-MAC 600).

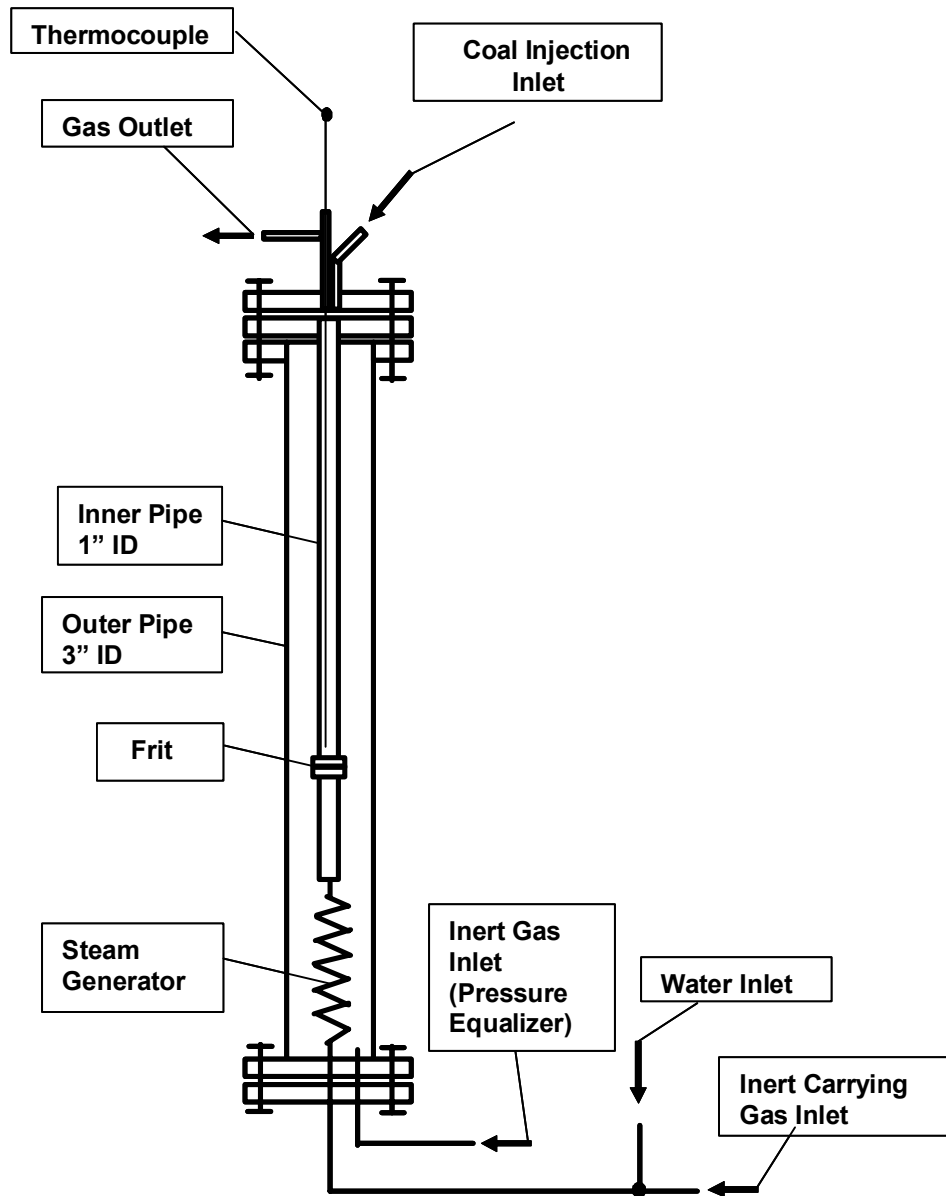


Figure 4 Schematic of the Fluidized Bed Reactor

RESULTS AND DISCUSSION

Thermogravimetric Analysis

CO and H₂ oxidation by Fe₂O₃

Theoretically, reduction of hematite to metallic iron results in a 30 % weight loss. TGA experiments on iron oxide reduction were conducted in 10 % CO in N₂, 10 % H₂ in N₂ and 5 % CO and 5 % H₂ in N₂. Figures 5, 6 and 7 contain the kinetic data on the iron oxide weight loss in 10 % CO in N₂,

10 % H₂ in N₂ and 5 % Co and 5 % H₂ in N₂, respectively, at temperatures ranging from 700 to 900 °C. It can be seen in Figures 5 and 6 that the rates of reduction with hydrogen are significantly faster than that with carbon monoxide. For example, the rate of initial percent weight loss at 900 °C in CO was 0.05 %/min, while that in H₂ was 0.28 %/min, which is nearly 6 times that in CO. Similar observations were made by Moon and Rhee (1997, 1998). The rate of initial weight loss percent of Fe₂O₃ in a mixture of 5 % H₂ and 5 % CO in N₂ at 900 °C was estimated to be 0.069 % /min. The effect of temperature on the oxidation rates of CO and H₂ by hematite is also clearly illustrated in these figures. Increase in temperature increases the overall rate of reduction. While complete reduction to hematite is not observed in the first 170 minutes of the reaction for temperatures upto 750 °C in 10 % CO, the conversion approaches 100 % at 800 °C and the theoretical 30 % weight loss is obtained at higher temperatures within 170 minutes. Multiple rate controlling mechanisms are observed for reactions with CO. The different stages are more visible at low temperatures (700 – 800 °C). Four different rate regimes are clearly seen for reactions at 750 °C with CO (Figure 5) and at 700 °C with the mixture of CO and H₂ (Figure 7). For the reaction with CO, it is seen that the initial weight loss takes place at a rapid rate to around 5 % and continues to reduce till around 7.5 % at a slightly slower rate. Theoretically, the complete reduction of hematite to magnetite is around 3.33 % while that from hematite to wustite is 10 %. Thus, this initial region can be assumed to be due to the reduction of hematite to wustite. This is followed by a rather slow rate of weight loss which is attributed to the change in crystallographic structures (from the rhombohedral structure of Fe₂O₃ to the the cubic structure of Fe₃O₄ and FeO) thereby suspending/significantly slowing down the reduction reactions. Rapid reaction was again observed in the third regime. This is attributed to the surface reaction controlled reduction of wustite to metallic iron. Finally the fourth region (with slower reduction kinetics) is hypothesized to be pore-diffusion controlled reduction of wustite once all the surface molecules are reduced. Due to the much faster reaction kinetics, all these regions are not visible in the reduction reactions with hydrogen at temperatures greater than 700 °C. In a reducing atmosphere containing H₂ near complete conversion is observed within 15 minutes of the reaction. Although the initial rates increased with temperature, the maximum overall reduction rate of hematite in H₂ was observed at 750 °C, decreasing thereafter with temperature. The presence of iron is observed to promote the Boudouard reaction resulting in carbon deposition and thus an increase in weight is observed at longer reaction times (Figure 8) in reaction systems containing CO. Up to 210 % of the original iron oxide weight was observed as a result of the Boudouard reaction. The x-ray diffractogram (not shown) revealed that carburizing of metallic iron occurred to form Fe₃C. The rate of CO disintegration is observed to increase with the temperature of the reaction.

Since the success of this process is dependent on the ability of the solids to regenerate, one set of TGA experiments were conducted with the mixture of CO and H₂ wherein the iron oxide was reduced by the mixture and was the regenerated using air and reduced again. The TGA profile (Weight loss % vs time) is shown in Figure 9. It is observed that at 850 °C, the iron oxide is rapidly regenerated from its metallic form and the subsequent CO/H₂ oxidation activity is approximately identical to the fresh oxides.

Carbonation of CaO

Theoretically, the weight gained by complete carbonation of CaO is 78.57 % of the original weight. However at 300 °C, the weight gain observed (not shown) was only 10 % while that at 700 °C (not shown) was 37 %. Figure 10 shows the kinetic profile of the carbonation experiments on the TGA at 750, 800 and 850 °C. Since the Gibb's free energy at temperatures above 900 °C becomes positive, experiments were not conducted at these temperatures. It is seen in Figure 10 that the weight increase is around 50 %, i.e. ~64 % conversion.

Repeated calcination carbonation cycles were also conducted in the TGA. The weight change vs. time data is shown in Figure 11. It is observed from the Figure that while near complete calcination was achievable, the activity of the calcined material for carbonation decreased with each cycle.

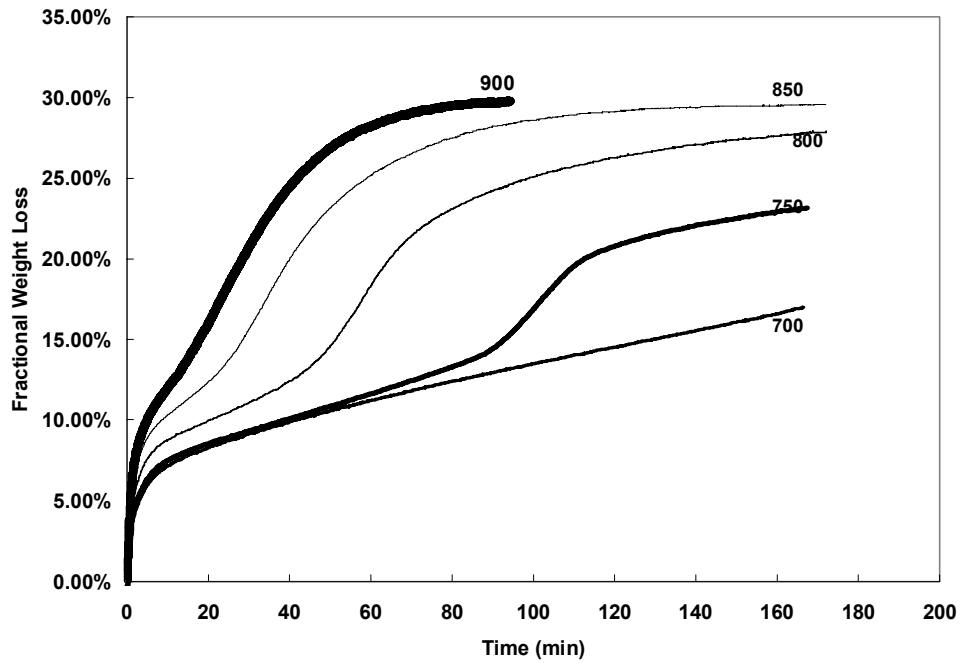


Figure 5 TGA Profile of Iron Oxide Reduction in CO

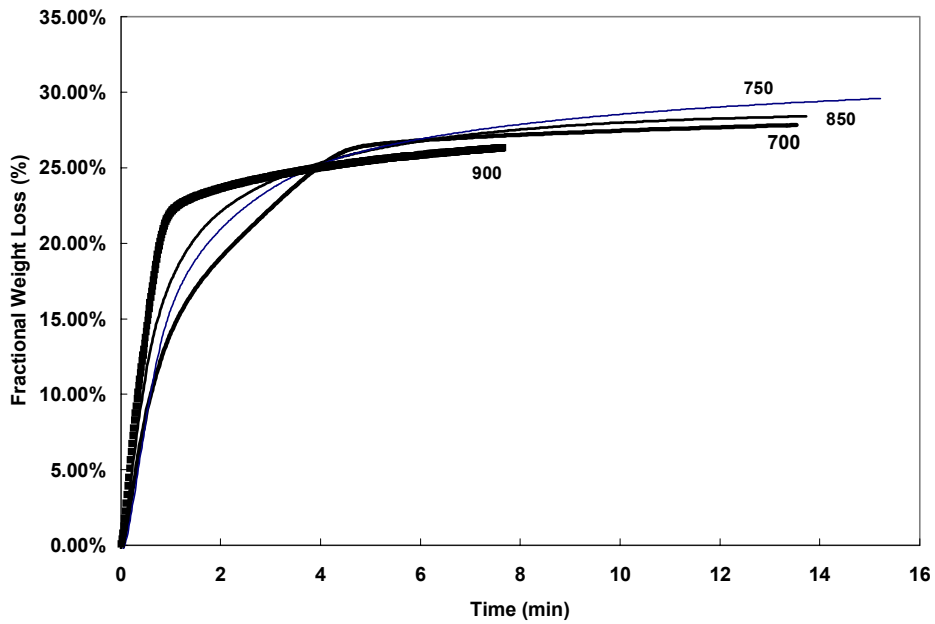


Figure 6 TGA Profile of Iron Oxide Reduction in H₂

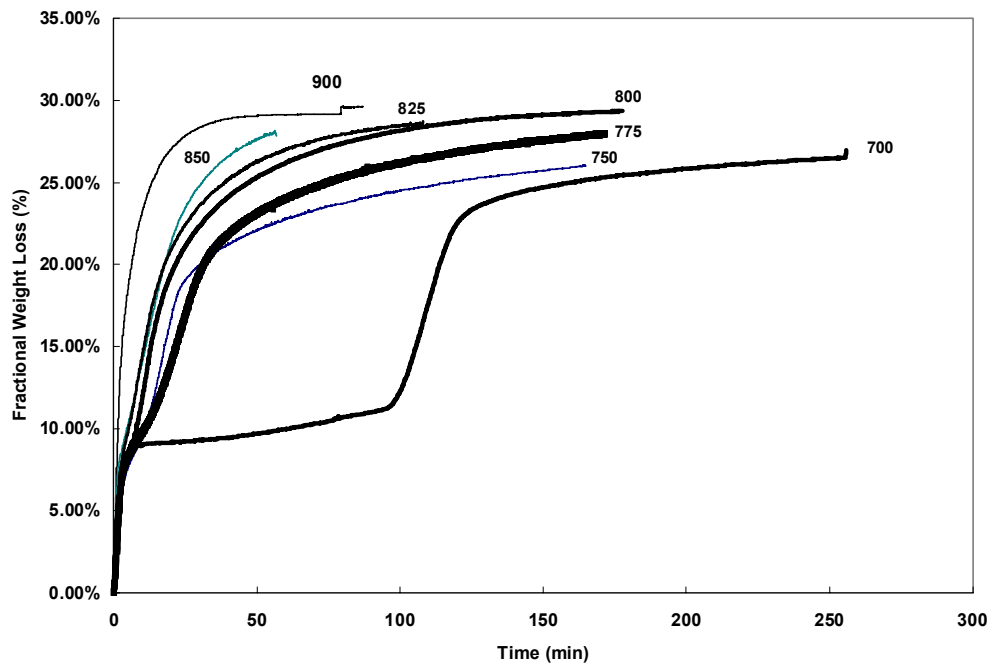


Figure 7 TGA Profile of Iron Oxide reduction in 5 % H₂ and 5 % CO mixture

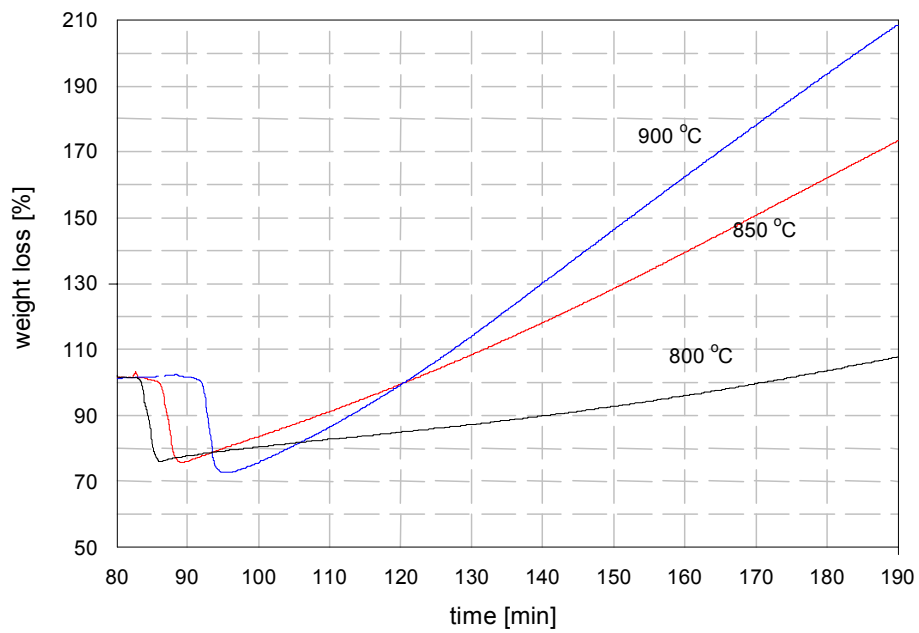


Figure 8 Evidence of Boudourd Reaction during Oxidation of CO by Hematite

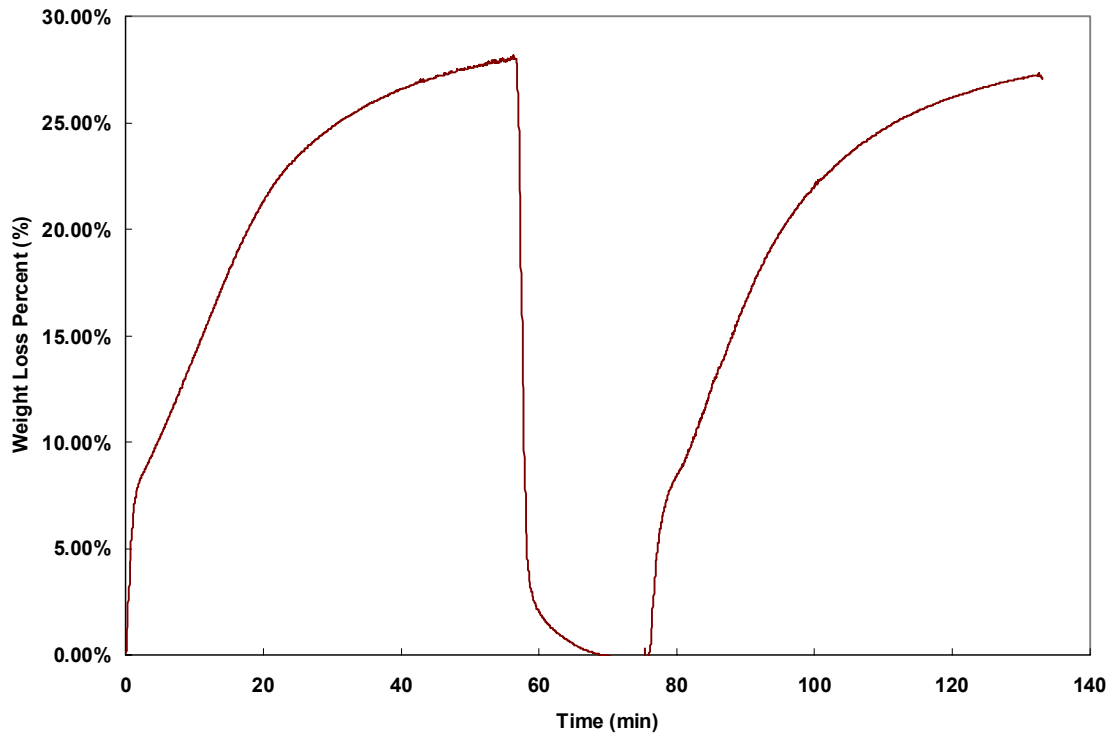


Figure 9 Oxidation reduction cycling of iron oxide in H₂-CO mixture and air

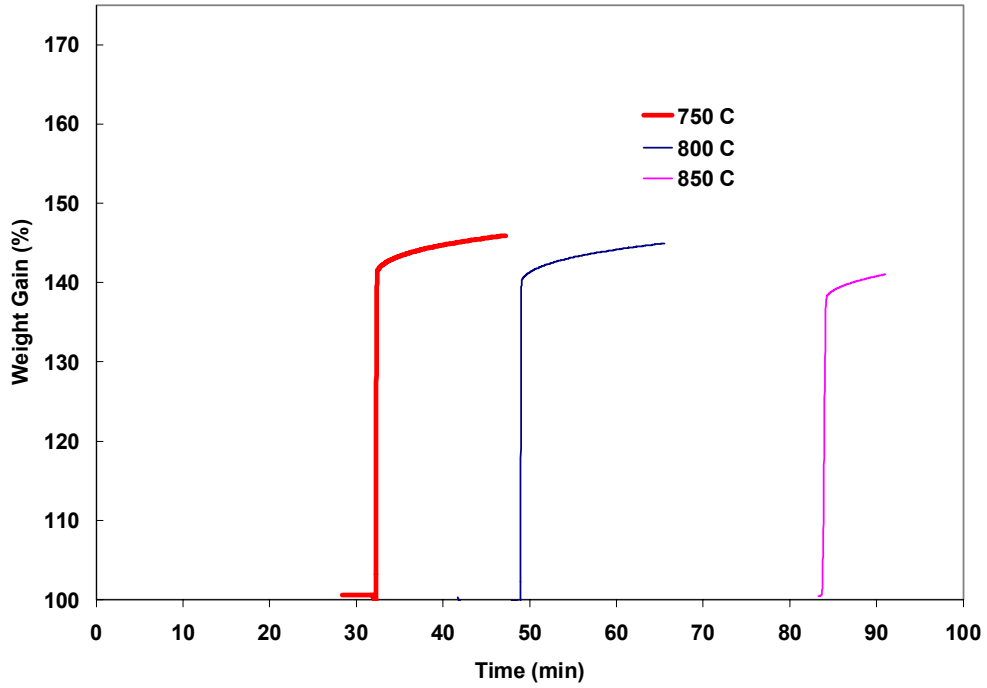


Figure 10 TGA profile of Carbonation of CaO

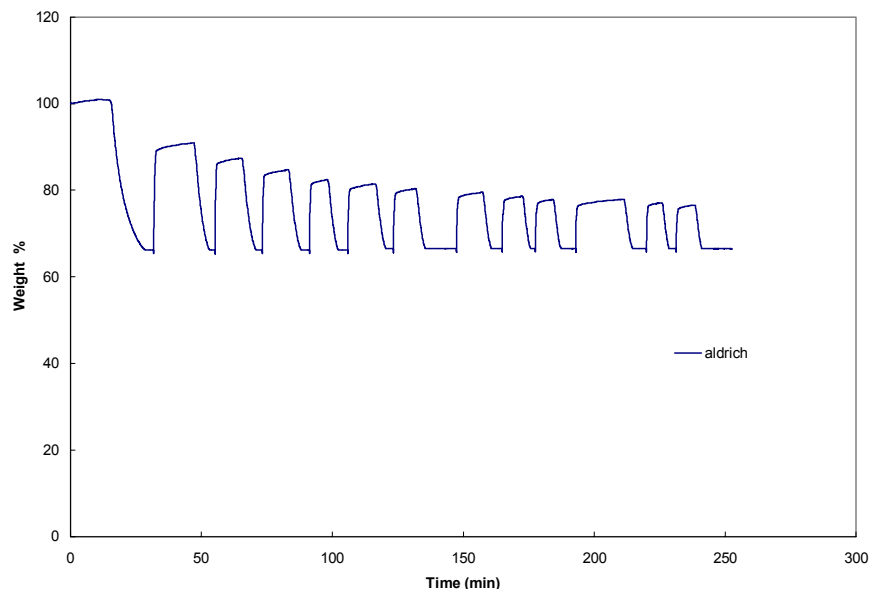


Figure 11 TGA profile of Calcination-Carbonation Cycling of CaCO_3 (obtained from Sigma - Aldrich)

Laboratory Scale Fixed Bed Studies

The influence of reaction temperature, steam content, and the loading of Fe_2O_3 and CaO on the rate of reaction and gaseous product profile was evaluated in a fixed bed reactor. All the data were analyzed based on the cumulative data obtained in 10 minutes.

Effect of temperature

Reaction temperature is an important parameter affecting the performance of coal gasification and subsequent water gas shift reaction. Gasification reactions are endothermic while the WGS reaction is exothermic. Thus, an optimal region of the reaction would produce the maximum gaseous yield with low CO content. This is clearly observed for equilibrium conditions in Figure 2 a. The effect of temperature in a fixed bed reactor was evaluated under two conditions: a) pyrolysis with nitrogen only and b) steam gasification (with a water flow rate of 1 mL/min).

During pyrolysis in N_2 , it is observed (Figure 12) that the cumulative CO_2 concentration at the end of 10 minutes decreases from 10 % at 750 °C to nearly zero at 900 °C. The CH_4 concentration is also observed to decrease (from 60 % at 750 °C to 19 % at 900 °C). The CH_4 content in the gas during pyrolysis is primarily a result of devolatilization of this component. However, the simultaneous decrease in both CO_2 and CH_4 with temperature may be explained as a result of the consumption of CO_2 during dry reforming of CH_4 as described by Eq [9] which is expected to increase with temperature. The dry reforming of CH_4 will result in an increase in the CO and H_2 content. It is seen from Figure 12 that CO and H_2 contents increase from 30 % to 80 % and 2 % to 20 %, respectively, when the temperature in the reactor is increased from 750 °C to 900 °C. The increase in the gasification, devolatilization and dry reforming rates partially contribute to the increase in CO and H_2 and the decrease in CO_2 concentration. The methane concentration increases at reaction temperatures greater than 900 °C to 73 % at 950 °C

while the CO₂ concentration is observed to be practically zero at this temperature. This is due to the complete consumption of the CO₂ produced by dry reforming and as a result the excess methane is not reformed. The CH₄ produced may be partially attributed to the methanation reactions of CO and C with H₂ (Eq 9 and 10). A corresponding decrease in CO and H₂ contents are also observed

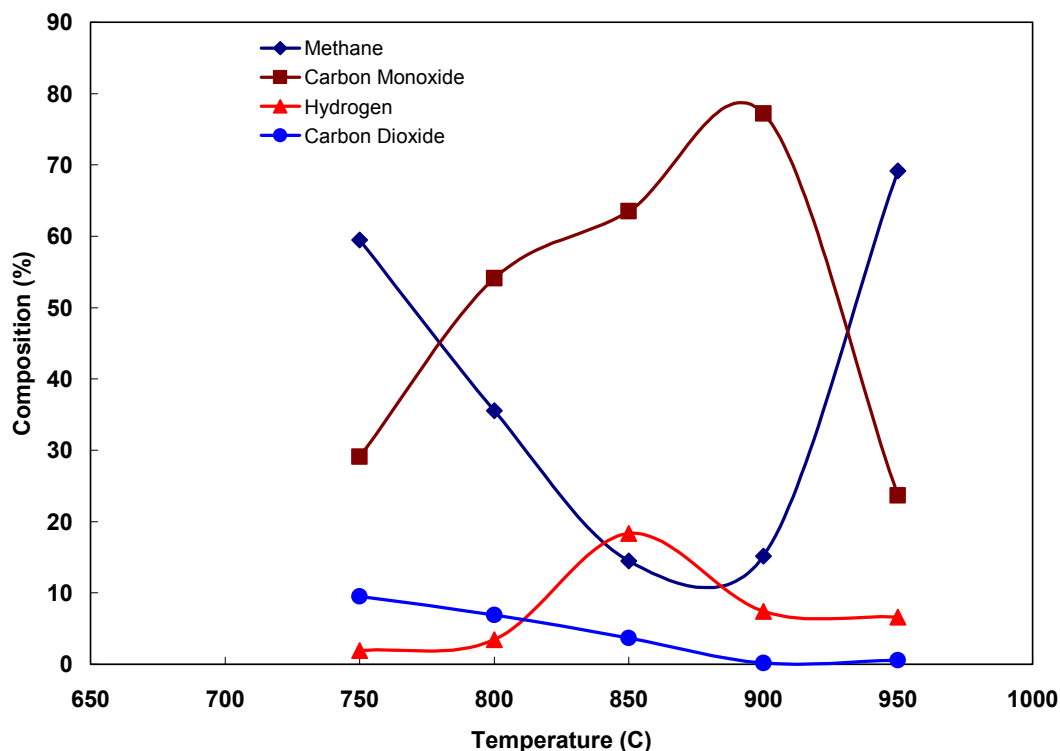


Figure 12 Influence of temperature on coal pyrolysis in N₂

In the presence of 91 % steam (Figure 13), the CO₂ concentration increases from 10 % to 22 % when the reactor temperature was increased from 700 °C to 850 °C. This was accompanied by an increase in H₂ concentration (2.5 % to 43 %) but only a moderate increase in CO content (30.5 % to 38 %) as compared to the results from experiments with no steam. The presence of steam increases the carbon conversion rates (Figure 14). For example, at 900 °C, a two fold increase in coal conversion is observed. The excess conversion is primarily due to steam reforming of the coal. In addition, the WGS reaction proceeds at much faster and as a result an increase in the CO production by gasification is reflected by the increase in CO₂ (due to WGS) in the overall product. The CH₄ concentration is also observed to decrease rapidly from 57 % at 700 °C to 8 % at 850 °C. However, this decrease is primarily due to steam reforming of methane. At reaction temperatures above 850 °C, the CO₂ concentration decreases while the CO content is observed to rise sharply primarily due to the predominance of CO₂ consuming reactions with an increase in temperature in comparison to the water gas shift reaction (which is exothermic). In addition, similar trends were also observed for experiments with different steam partial pressures. However, the H₂ and CO₂ contents were found to increase with water flow rate (steam to fuel ratio) while CO and CH₄ contents were found to decrease. For example, at 800 °C, the H₂ and CO₂ concentration were found to increase by 12 and 1.83 times, respectively while the CO and CH₄ concentrations were observed to decrease by more than half and one-third respectively when a water flow rate of 1 mL/min was employed as compared to the experiments with no steam. Similar findings

were also reported by Kim et al during their studies with coal gasification and Gil et al and Hofbauer with biomass gasification.

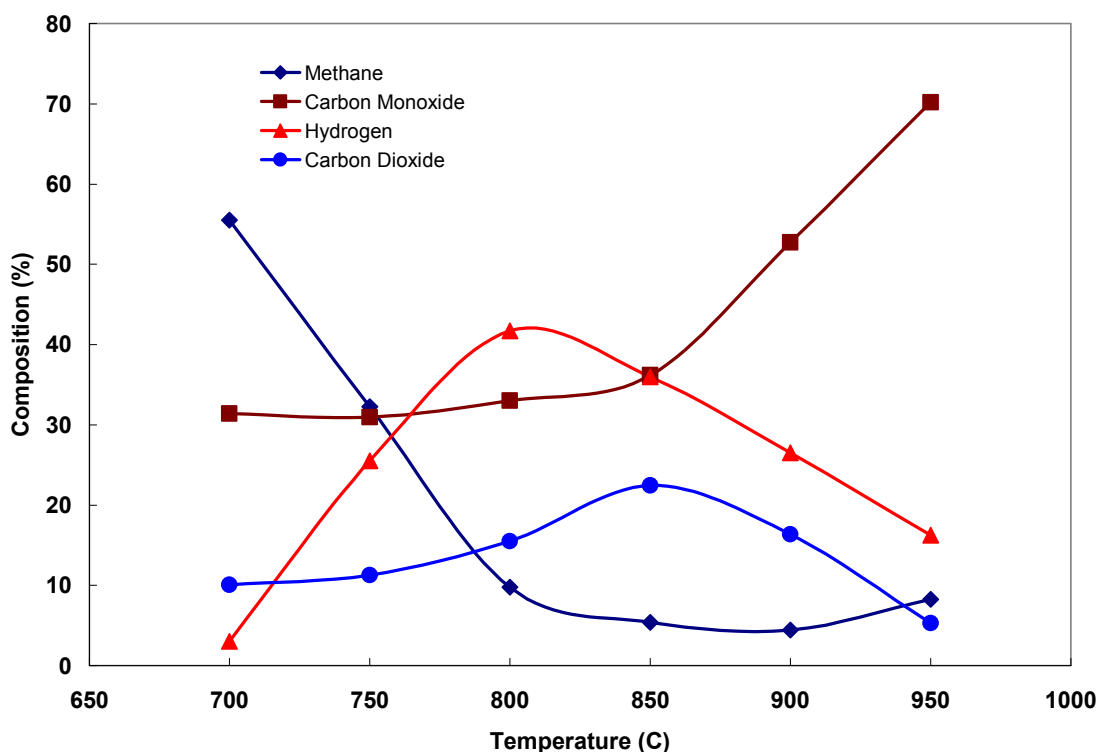


Figure 13 Influence of temperature of steam gasification of coal

Char yield, in principle, should be as low as possible to ensure high conversion during gasification. The rise in temperature led to an increase in the coal conversion (Figure 14). In general, it was observed that the conversions were higher in the presence of steam. Two regimes of conversion were observed for experiments with and without steam. When steam was present in the reactor system, the increase in conversion was 99 % when the temperature was raised from 700 to 800 °C but increased by an additional 99 % at 900 °C. The transition temperature for coal pyrolysis experiments in nitrogen was around 900 °C. Three processes are mainly responsible for the increase in gas yield with temperature (a) greater production of gas in the initial pyrolysis (which is faster at higher temperatures, (b) steam cracking and reforming of tars (which also increases with temperature) and (c) endothermal reactions of char gasification. The results show that for the given coal, gasification should be carried out at temperatures in the range of 800 – 900 °C.

A first order rate of reaction was assumed to calculate the rate constant. Figure 15 is a plot of $\ln(C/C_0)$ vs. time where C and C_0 are the dynamic and initial mass of coal. A theoretical first-order plot should pass through the origin, however, as seen in the figure, this criterion is not obeyed for the presented set of data which suggest that perhaps the reaction mechanism is somewhat complex due to rapid decomposition of coal volatile matter and the differences in the gasification rates of coal, char and semichar. Linear plots of $\ln C/C_0$ vs time data are however observed. The estimated rate constants at 850°C (0.0051 min^{-1}) and 900 °C (0.0078 min^{-1}) were about two and three times the value for the rate constant obtained at 800 °C (0.0031 min^{-1}), respectively. Arrhenius parameters, activation energy and frequency factors were estimated to be 663.7 J mol^{-1} and 1.05 min^{-1} , respectively. It must be noted that the evaluation of absolute reactivities is not possible based upon the data obtained alone, since the coal

reacts with steam, the reactivity in addition to being temperature dependent could also be a function of the amount of steam used.

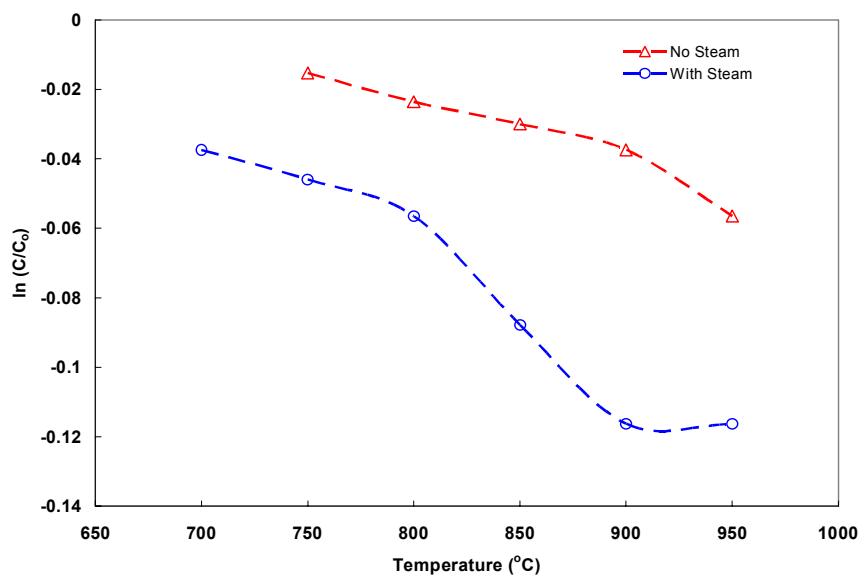


Figure 14 Conversion (residence time = 10 minutes) as function of temperature.

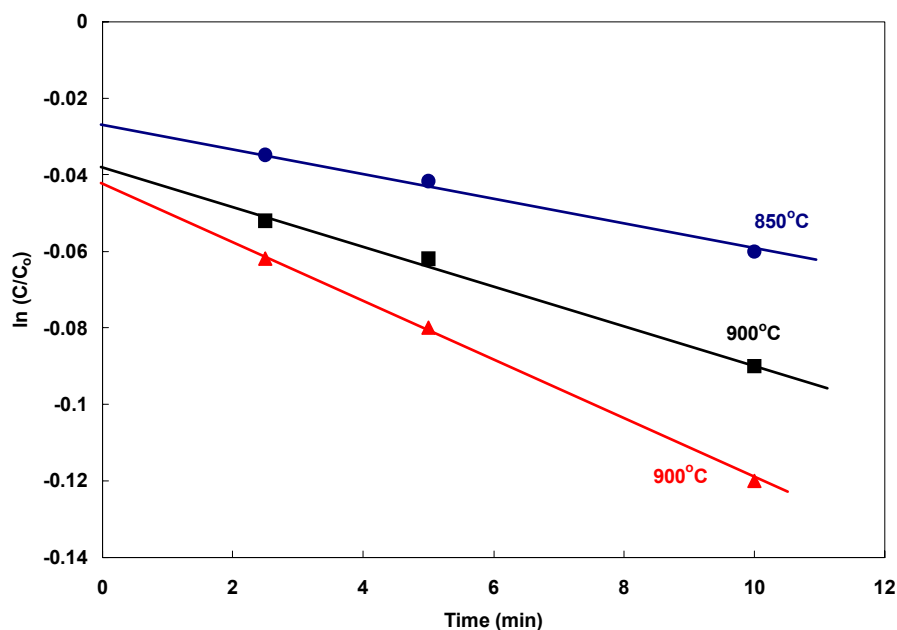


Figure 15 Plots for the determination of rate constants

Effect of Steam

The effect of the partial pressure of steam was also studied by increasing the water flow rate without adding any iron oxide at 850 °C. The cumulative volumetric data of the gases were calculated based on a residence time of 10 minutes. It is seen in Figure 16 that on increasing the water flow rate to 0.5 mL/min (85 %), both the CO and CO₂ contents increased by 77 % and 80 %, respectively, while those of H₂ and CH₄ decreased by 39 % and 50 %, respectively. In this regime, steam reforming of coal

and methane predominate and the steam is not sufficient for extensive WGS and as a result the CO content is observed to increase sharply while that of H₂ decreases. However, on further increasing the steam partial pressures to 91 % (1 mL/min of water), the CO content decreases from a maximum of 58 % to 43 % at 91 % steam partial pressure. Simultaneously, the H₂ content increased indicating the required flow rate of steam was obtained for water gas shift reaction to predominate. At value of water flow rate greater than 1.3 mL/min (95 % steam), no change in the outlet gas compositions were observed. Figure 17 contains the data on coal conversion rates. It is clearly seen from the figure that the addition of steam significantly enhances the conversion rates upto a value of 1.3 mL/min. A 282 % increase in the coal conversion was observed when the water flow rate was increased from 0 to 1.3 mL/min. Based on the data it is concluded that greater than 91 % steam should be used for maximizing the hydrogen yield and content via the WGS reaction

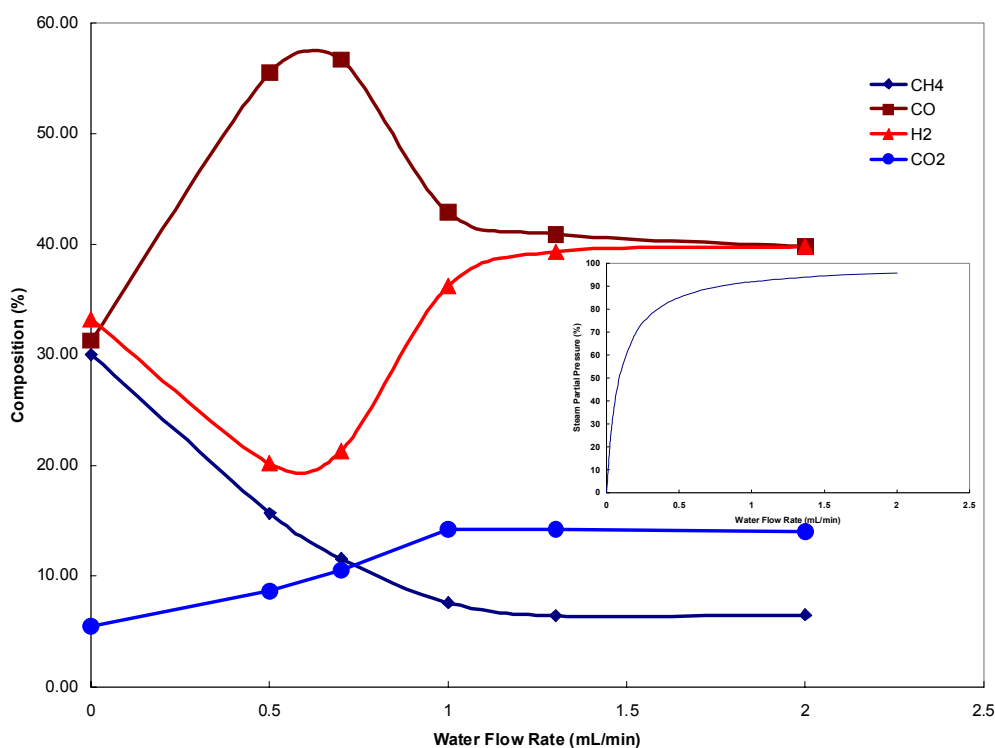


Figure 16 Effect of steam content (based on water flow rate) on product profile (Inset – steam partial pressure vs water flow rate)

Effect of Solid Oxygen Carrier Loading

Iron oxide is known to be an effective water gas shift catalyst. In addition, it also serves as an oxygen supplier to, not only convert the CO to CO₂, but also, partially combust the carbon. To study the effect of the oxygen carrier loading on the product composition, experiments were conducted at several loadings at a temperature of 850 °C and a water flow rate of 1 mL/min (91 % steam). The data obtained are presented in Figures 18 and 19. It is seen in Figure 18 that an increase in the iron oxide to coal ratio resulted in an initial increase in hydrogen, and carbon dioxide concentrations while a decrease in the CO content and CH₄ content is observed. An increase in the iron oxide to coal ratio from 0 to 5 resulted in a 167 % increase in the hydrogen content to 56 %. In the same range of iron oxide to coal ratio, a decrease in the CO content from 57 % to 3 % was observed. Previous researchers have found that an

increase in the O₂ supply resulted in a decrease in the H₂ content and an increase in the concentrations of CO and CO₂. This contradicting data at lower iron oxide:coal is a result of enhanced water gas shift reaction that results in an increase in the H₂ content and a decrease in the CO content. The CO content is further decreased by the direct oxidation of CO by Fe₂O₃. The CO₂ content shows a corresponding increase. However, on increasing the iron oxide to coal ratio was increased to a value greater than five, a decrease in H₂ concentration was observed while a sharp increase in the CO content occurred. The decrease in H₂ content for experiments employing a Fe₂O₃:coal ratio greater than five is due to the oxidation of H₂ to steam. This decrease in the H₂ content is reflected in a corresponding increase in the relative CO concentration even though CO is also oxidized by iron oxide (albeit at a slower rate). The CO₂ content in the product stream decreased gradually after reaching a maximum value when the Fe₂O₃:coal ratio of 2.5. As described earlier, the decrease in CO₂ is a result of dry reformation of methane and is confirmed by the gradual decrease in the methane content. In addition, it is possible that methane is partially oxidized to CO and H₂ in the presence of excess Fe₂O₃. The possibility of methane decomposition using Fe₂O₃ is investigated by evoking the following chemistry. It is hypothesized that methane is decomposed by both of oxygen radical (O·) and oxygen anion (O⁻). The oxygen radical is produced by thermal decomposition of water. It is considered that oxidative decomposition of methane progresses by oxygen radical via the following reactions.



The net reaction is

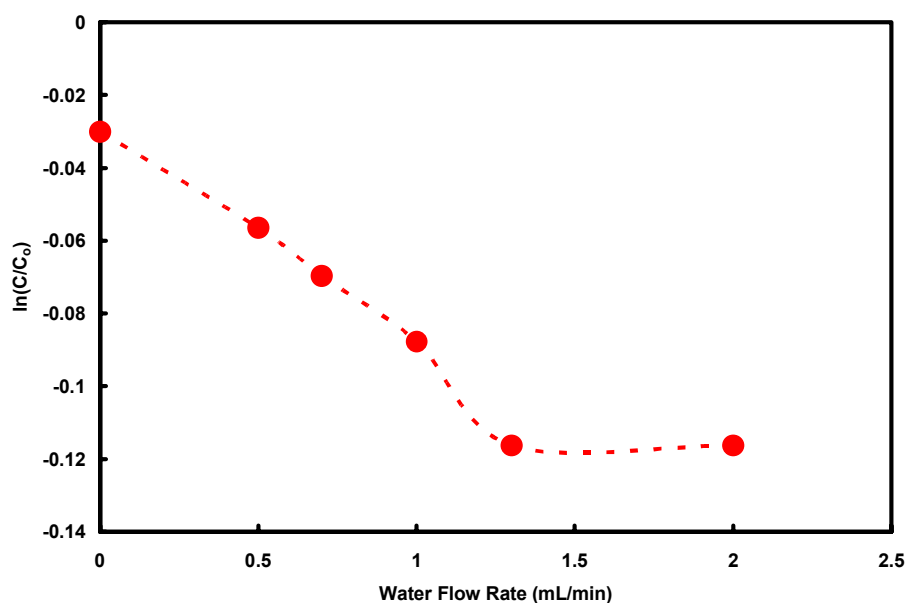


Figure 17 Influence of steam content (water flow rate) on conversion.

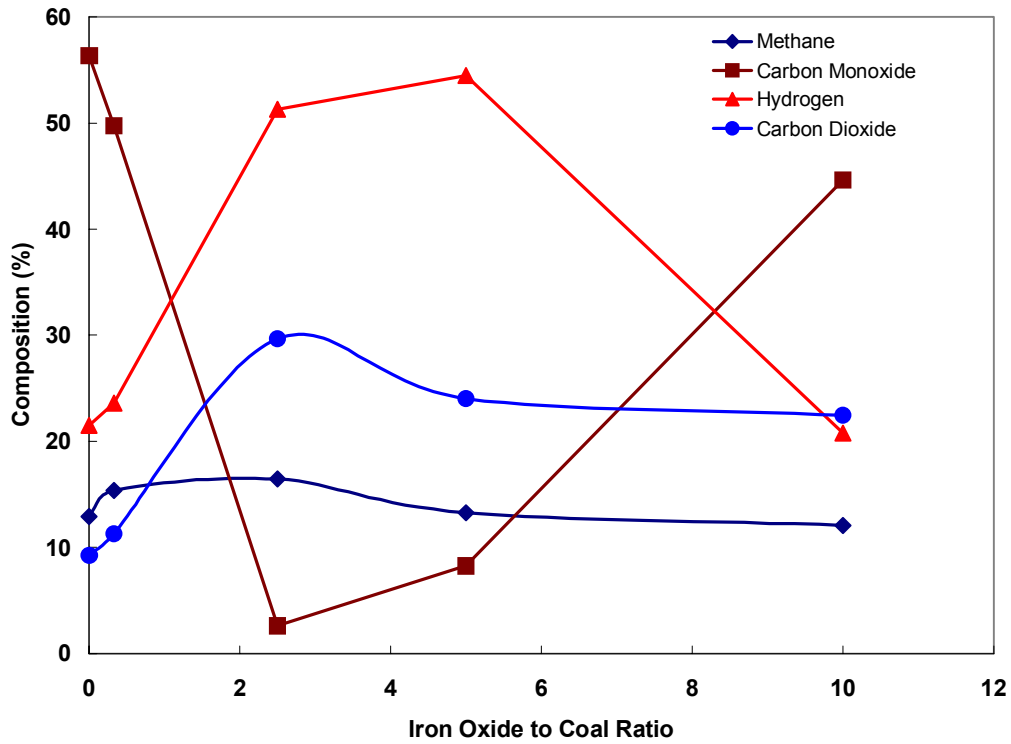


Figure 18 Effect of iron oxide loading on gasification product profiles

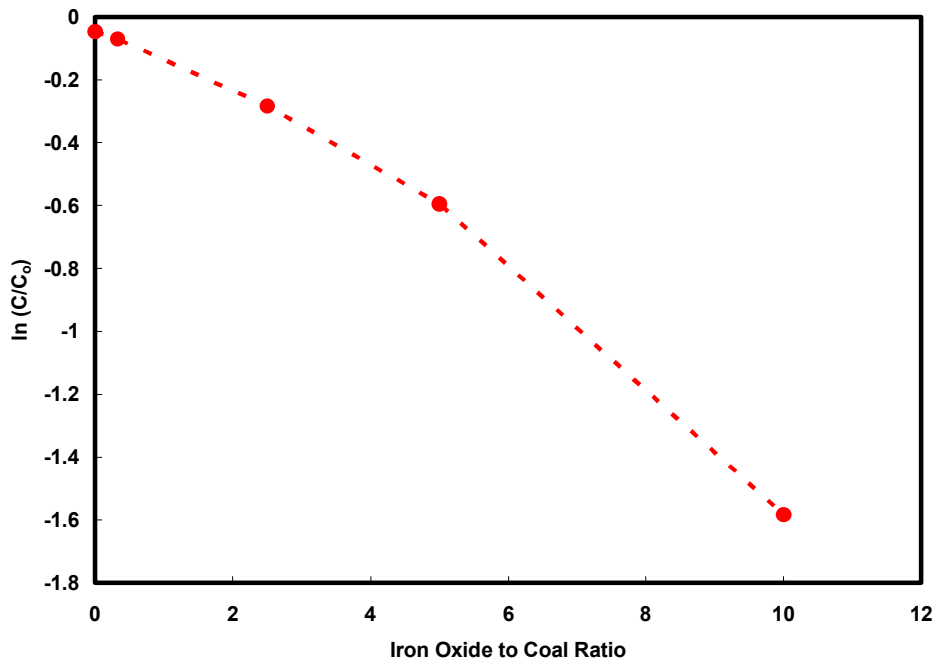
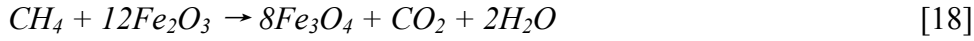
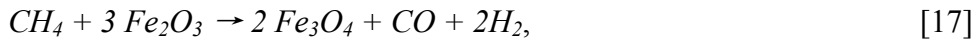


Figure 19 Effect of iron oxide loading on coal conversion

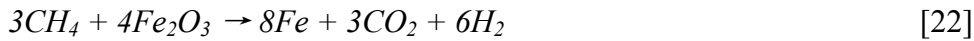
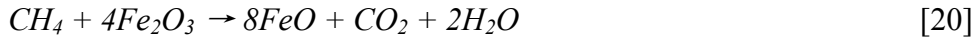
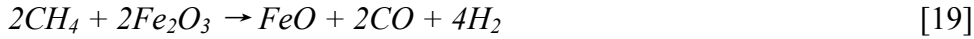
Oxygen anion could be produced during the reduction of Fe₂O₃ crystal. For example,



The following overall reactions also occur



Furthermore, Fe₂O₃ is possible to reduce to FeO and Fe.



The free energy change and equilibrium constants at 825 °C, for reaction [15] and reactions [17] through [22] are listed in Table 1. It is observed that the reactions are favoured thermodynamically at these temperatures. On the other hand, the equilibrium conversion of the reactions is expected to decrease with increasing pressure. The data, however, shows that reaction [15] does not progress in the absence of a suitable catalyst although thermodynamic analysis does show that the reaction is favorable. In the oxidative methane decomposition processes using oxygen anion into the iron oxide, the equilibrium constant of reaction [19] is found to be the largest of all the equilibrium constants for reactions [17] through [22].

Table 1 Gibbs Free Energies of reactions 15 - 22

Eq #	Reaction	ΔG_{1098K} (kJ/mol)	K	Effect of P
[15]	CH ₄ + H ₂ O → CO + 3H ₂	-1000	3.66X10 ⁴⁷	-
[17]	(1/3)CH ₄ + Fe ₂ O ₃ → (2/3) Fe ₃ O ₄ + CO + (2/3)H ₂	-53	348	-
[18]	(1/12)CH ₄ +Fe ₂ O ₃ →(2/3)Fe ₃ O ₄ +(1/12)CO ₂ +(1/6)H ₂ O	-38	67	-
[19]	CH ₄ + Fe ₂ O ₃ → (1/2) FeO + CO + 2 H ₂	-266	4.65X10 ¹²	-
[20]	(1/4) CH ₄ + Fe ₂ O ₃ → 2 FeO + (1/4) CO ₂ + (1/2) H ₂ O	-120	4.96X10 ⁵	-
[21]	3CH ₄ +Fe ₂ O ₃ → 2Fe + 3CO + 6H ₂	-209	8.88X10 ⁹	-
[22]	(3/4) CH ₄ + Fe ₂ O ₃ → 2 Fe + (3/4) CO ₂ + (3/2) H ₂	-74	3281	-

The conversion of coal increased with an increase Fe₂O₃:coal ratio while the char formation (as determined by the carbon in the product gases) decreased (Figure 19). The coal conversion improved greater than 17.5 times when the iron oxide to coal ratio was increased from 0 to 10. Although the coal conversion improved significantly, it was observed (Figure 18) that the hydrogen purity is significantly compromised along with a rise in the CO content. Based on this set of data it can be concluded that the optimal ratio of Fe₂O₃:coal should be between 2.5 and 5. At these values, the conversions are increased by 4.7 and 8.5 times as high as the case when no iron oxide was added. The $\ln(C/C_0)$ vs $Fe_2O_3:coal$ ratio appears to be fairly linear. It can be represented as

$$\ln \frac{C}{C_0} = -k \frac{[Fe_2O_3]_0}{C_0}$$

Differentiating and rearranging the above equation we obtain

$$\frac{dC}{d[Fe_2O_3]_0/C_0} = -kC$$

We can deduce from the above information that not only does Fe_2O_3 enhance the conversion rates (including carbon conversion and devolatilization) but it does so in the manner of a catalyst rather than a reactant. However, the monotonous increase of carbon in the outgases while the CH_4 content remained fairly constant indicates that the sum of CO and CO_2 yield is directly proportional to the Fe_2O_3 :coal ratio or

$$\frac{dCarbon}{d[Fe_2O_3]/C_0} = -k[Fe_2O_3]/C_0$$

Thus, it can be concluded that iron oxide causes some oxidation of carbon. The rate constants of steam reforming of coal with (Fe_2O_3 :coal =0.065) and without iron oxide were determined assuming that the steam reforming of coal can be modeled by the first order reaction kinetics. A linear plot of $\ln (C/C_0)$ vs *time* data was observed. The estimated rate constant at 850 °C was 0.0523 min^{-1} , which increased to 0.124 min^{-1} . The data show that while the reaction proceeded faster at 850°C as compared to the condition when no iron oxide was added, the coal conversion rates were slower at 950°C.

Effect of addition of Calcium Oxide

The addition of calcium oxide in the reaction mixture drastically improved the purity of H_2 and the conversion at the end of 10 minutes. Figures 20 and 21 contain the data on the composition of the product gases and coal conversion, respectively. Greater than 70 % purity of hydrogen was achievable with more than 50 % conversion at a CaO:coal of 48. It must be noted that the conversion was only 4.7 % when no CaO was added. Thus, the addition of 50 times as much CaO as compared to the carbon improved the conversion by more than 18 times which was further improved by nearly twice when the ratio of CaO: coal was increased to 80. When a ratio of 80 was employed, the conversion increased to 89 % with 61 % hydrogen in the product gases. The maximum hydrogen purity observed with simple coal gasification was 40 % which increased to a maximum of 55 % due to the addition of iron oxide. In the experiment conducted with a CaO:coal ratio of 48, the methane and the CO content was found to be the minimum. Thus, the addition of CaO removes the thermodynamic limitation posed on the water gas shift reaction to increase the H_2 purity. The CO content decreased (from 42 % without any CaO addition to 17 % when the ratio used was 48) due to the removal of CO_2 from the gases by CaO. The increase in the extent of the WGS resulted in the production of more hydrogen and CO_2 . The decrease in CH_4 content is attributed to the dry reforming of methane on the CaO by CO_2 . The CO_2 captured by the CaO is released and adsorbed dynamically at these temperatures. The CH_4 molecules in the vicinity of $CaCO_3$ is reformed by the CO_2 released by these sites (Eq.[9]). However, when a CaO:coal ratio of 80 was employed, the concentration of $CaCO_3$ sites on the surface decreased, thereby decreasing the degree (probability) of methane dry reforming. As a result, it is observed that the CH_4 content increased at these ratios. Although 90 % of the carbon in coal was found to have reacted, the carbon in the exiting gaseous product was found to be only 0.023 g (Figure 21) which represents only 19 % of the total C gases formed. The remaining C was captured in the form of $CaCO_3$ in lime.

Figure 22 shows a typical profile product composition as a function of time. The experiments were conducted at 670 °C, with 1 mL/min water flow rate, and Fe_2O_3 :coal and CaO:coal ratios of 2 and 50 respectively.

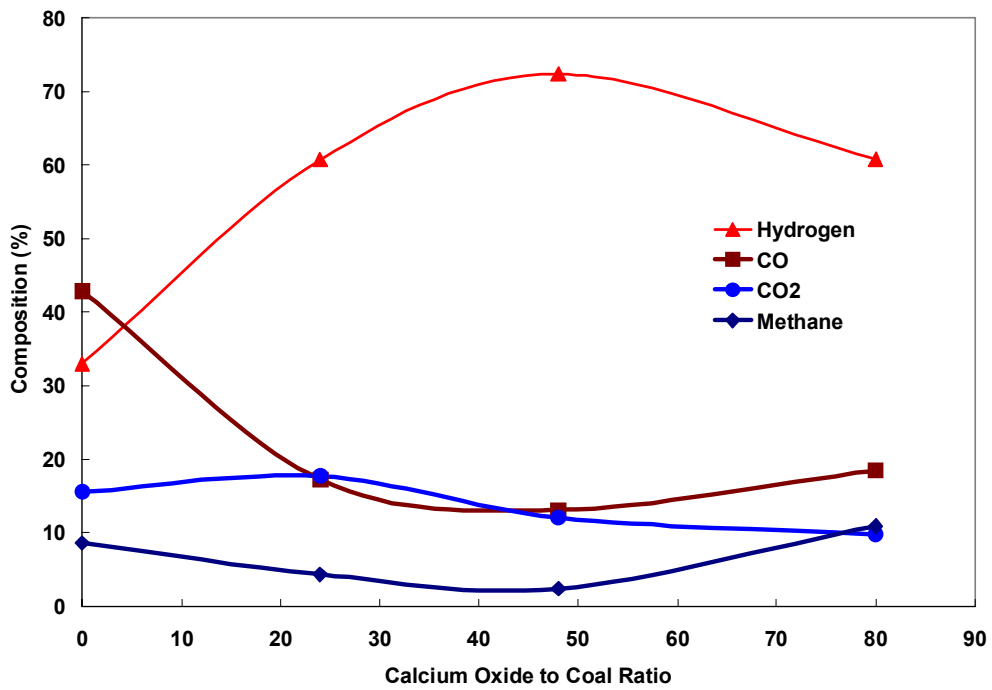


Figure 20 Effect of calcium oxide loading on gasification product profiles

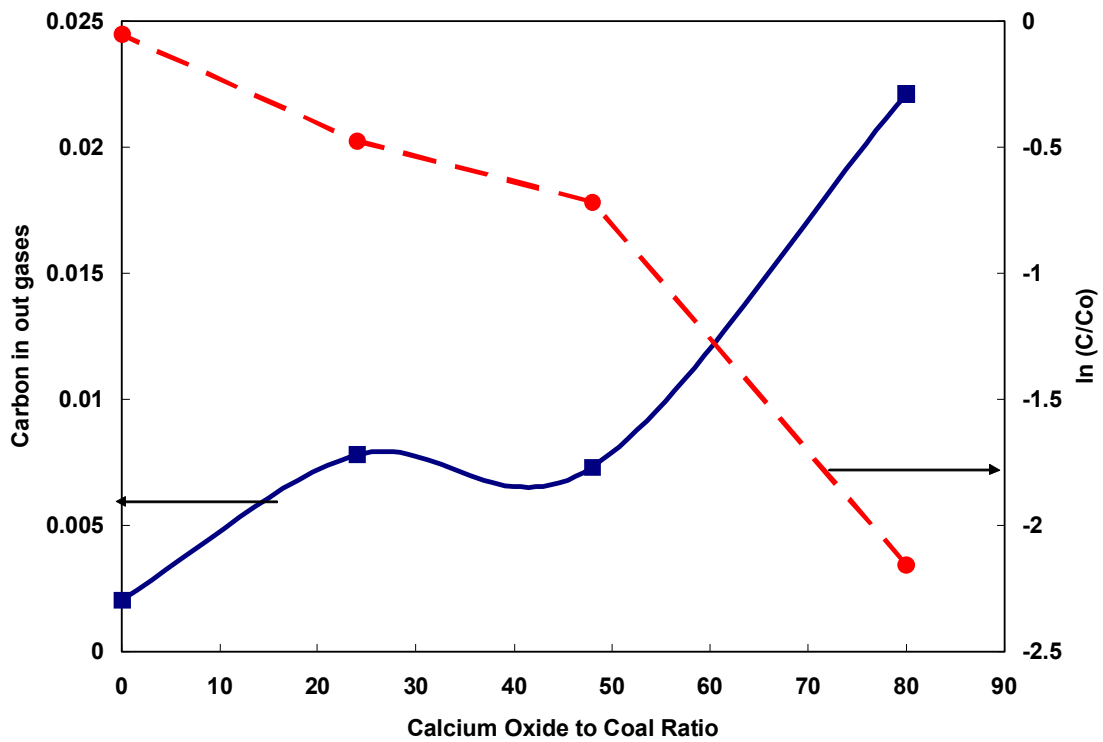


Figure 21 Effect of calcium oxide loading on coal conversion and carbon in the product

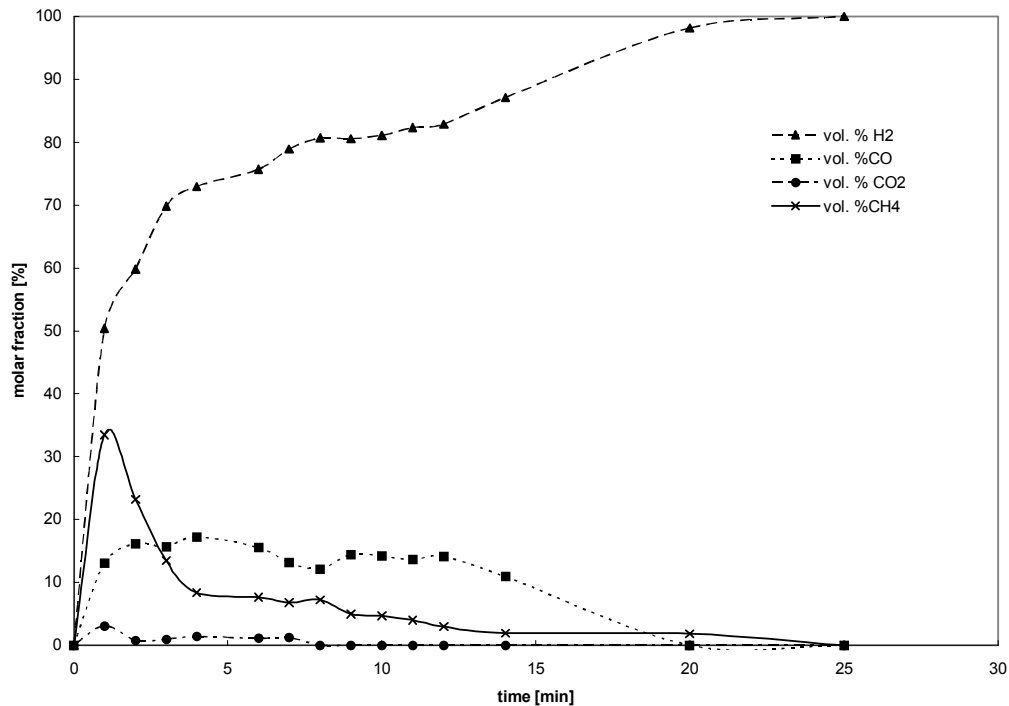


Figure 22 Typical product distribution as a function of time in a fixed bed reactor

Fluidized Bed Studies

Preliminary experiments were conducted in a fluidized bed reactor. 2 g of coal was added to 60 gms of solids. The solids were fluidized at 15 times the minimum fluidization velocity (based on previous studies). Silica sand was added as the filler material to make up the solids mass. Figure 23 shows the product profile and the total gas output under different steam partial pressures at 670 °C. Only sand was used as the fluidized solids. A gradual rise in the total gas output is observed with an increase in steam partial pressure up to 75 % steam. A sudden increase is observed when the steam pressure is increased to 85 %. The hydrogen content, however, does not change (61 %) when the steam partial pressure is increased from 75 % to 85 %. Both methane and CO decrease with the increase in the amount of steam present in the reactor. Steam reformation of the produced methane is primarily responsible for the decrease in the CH₄ content in the product gases while an increase in the water gas shift reaction causes the decrease in the CO content with steam pressure. This is accompanied by an increase in the CO₂ content which decreases at higher steam contents. The results show that 85 % steam is ideal for these studies. Higher steam partial pressures caused operational problems.

The effect of temperature on the product gas profile and the total gas output at steam partial pressure of 75 % is shown in Figure 24. The total gas produced at the end of 15 minutes increases drastically at temperatures above 770 °C. A maximum hydrogen content (61 %) was obtained at 770 °C, which decreased to 54 % at 870 °C. It is known that at 900 °C, the calcinations of CaCO₃ is favored over the carbonation of CaO. This results in the reduction of CO₂ removal capacity of the CaO and is reflected in the sudden increase in the CO₂ content at 870 °C. Rates of methane reformation reactions, on the other hand, was observed to increase. Nonetheless, the high gas output (due to coal conversion) at 870 °C meant a higher yield of hydrogen and has been considered suitable for further studies.

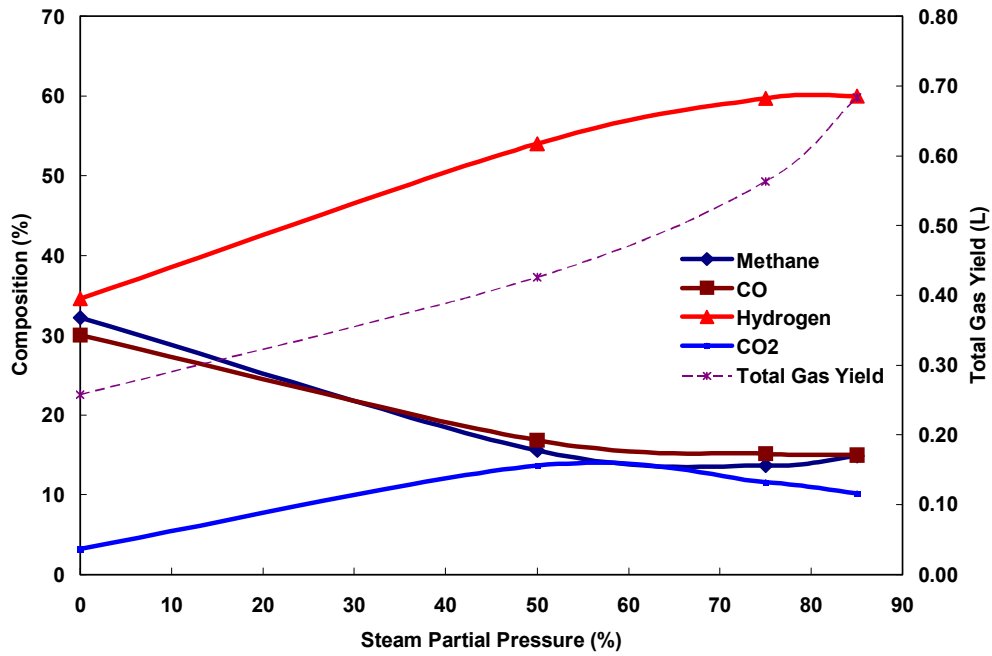


Figure 23 Product characteristics as a function of steam partial pressure in a fluidized bed reactor

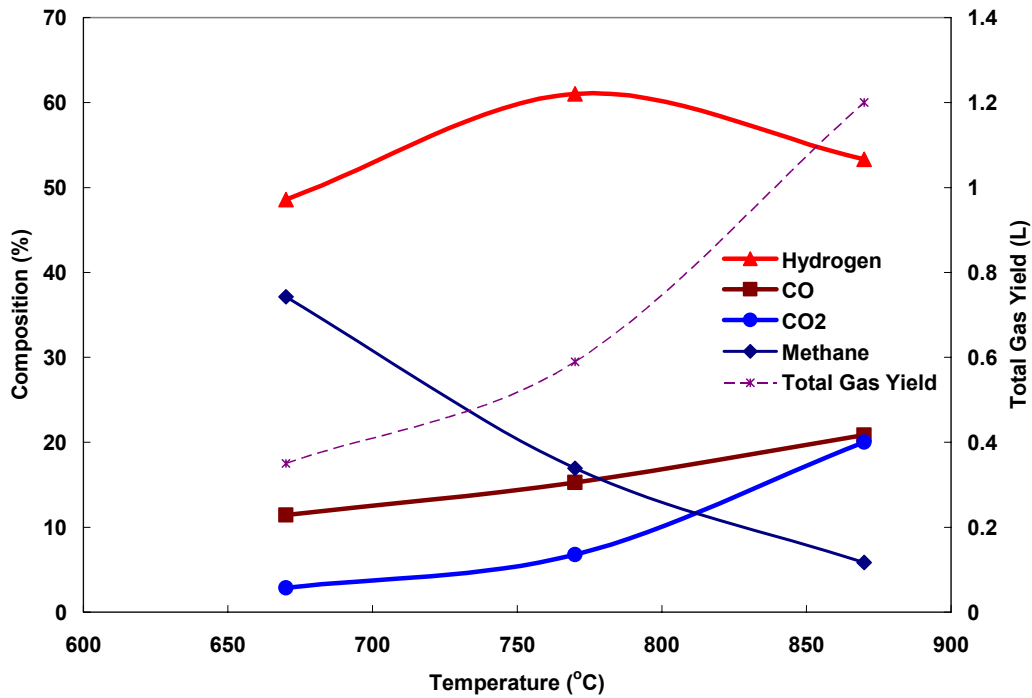


Figure 24 Product characteristics as a function of temperature in a fluidized bed reactor

Figure 25 contains the data on the product profile and the total gas output as a function of iron oxide loading at 770°C and 85 % steam. 40 g of CaO was used for these studies. It is observed that the hydrogen content decreased by 14 % on increasing the iron oxide content in the reactive mixture from

20 g to 30 g. A maximum of 70 % hydrogen was observed when 20 g of iron oxide was employed. On the other hand, the total gas output increased by only by 6 %. In addition the CO₂ and CH₄ contents were also observed to increase at the highest iron oxide loadings of 30 g. Thus 20 gms of iron oxide was found to be suitable for enhancing the conversion of CO to CO₂.

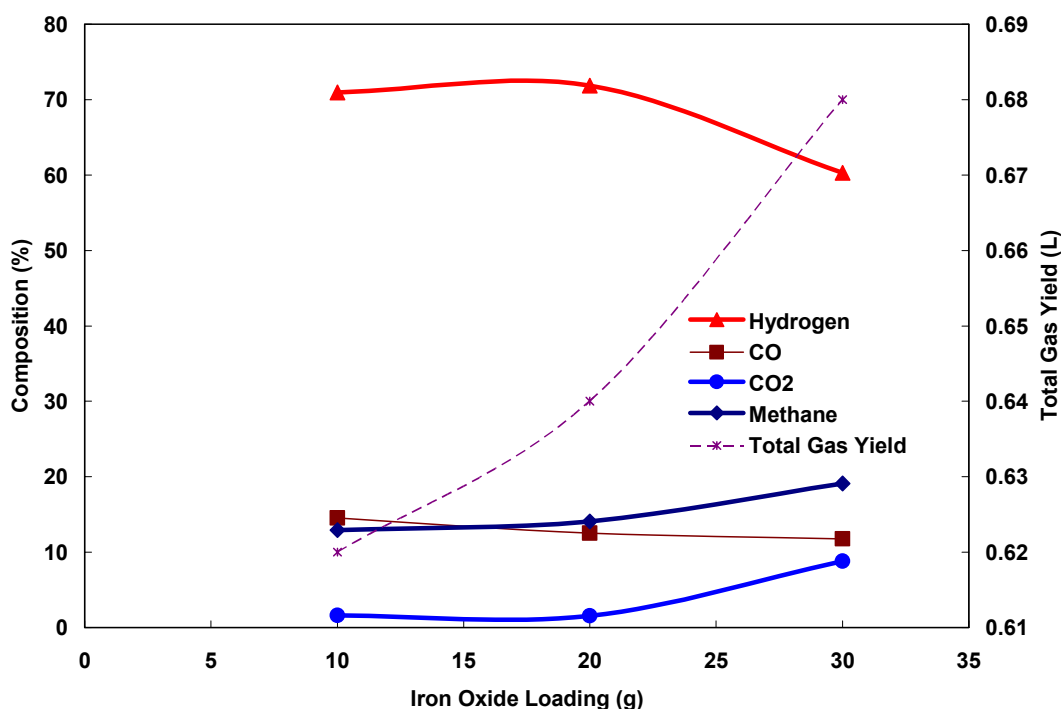


Figure 25 Product characteristics as a function of iron oxide loading in a fluidized bed reactor

The results from experiments conducted with 20 g of iron oxide and varying loads of CaO are shown in Figure 26. The temperature in the reactor was maintained at 770° C and 85 % steam was introduced for these experiments. Increasing the CaO loading was observed to have a positive effect on the hydrogen purity. As observed in the Figure, increasing the CaO loading from 10 to 20 gms resulted in 40 % enhancement in purity (from 50 % to 70 %). Simultaneously the CH₄ and CO₂ in the product gases is observed to decrease. Further increase in the CaO content did not significantly enhance the hydrogen purity. However, it improved the coal gasification characteristics by increasing the gas output by an additional 10 %.

CONCLUSIONS

The preliminary studies show that experiments conducted at 870 °C, 85 % steam with 40 g of CaO and 20 g of Fe₂O₃ would yield a gas with the highest hydrogen purity along with maximum coal conversion (Figure 27). The use of iron oxide alone had a negative effect on the hydrogen yield while the use of CaO alone increased the hydrogen yield and purity. In addition, the presence of CO₂ showed a strong negative correlation with CH₄. This is primarily due to the dry reforming of methane in the presence of CO₂. This is also corroborated with the positive correlation between CH₄ and CaO (since CaO may remove excess CO₂ resulting in the decrease in the extent of dry reforming of methane). The negative correlation observed between methane and iron oxide is significant in that iron oxide also helps in demethanation. In addition, it is observed that both iron oxide and the calcium oxides could be used

for multiple cycles without significantly losing its activity. The optimal temperature and steam partial pressures appear to be between 800 – 850 °C and 85 %, respectively. The Fe₂O₃:coal and CaO: coal ratios should be maintained in the ranges of 2.5 – 5 and ~50, respectively.

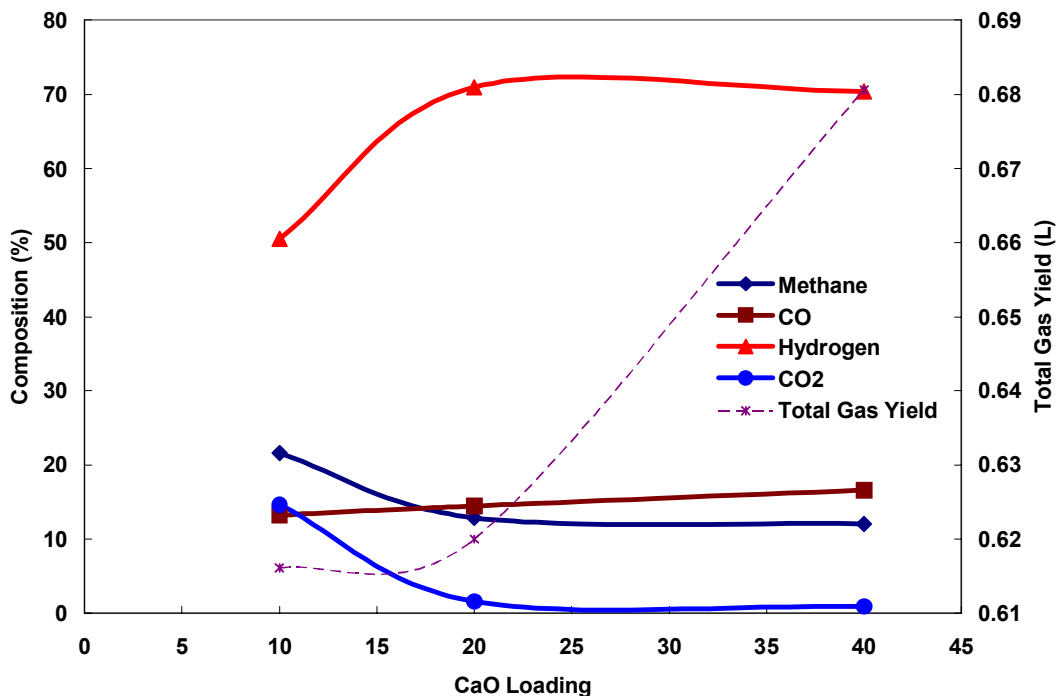


Figure 26 Product characteristics as a function of CaO loading in a fluidized bed reactor

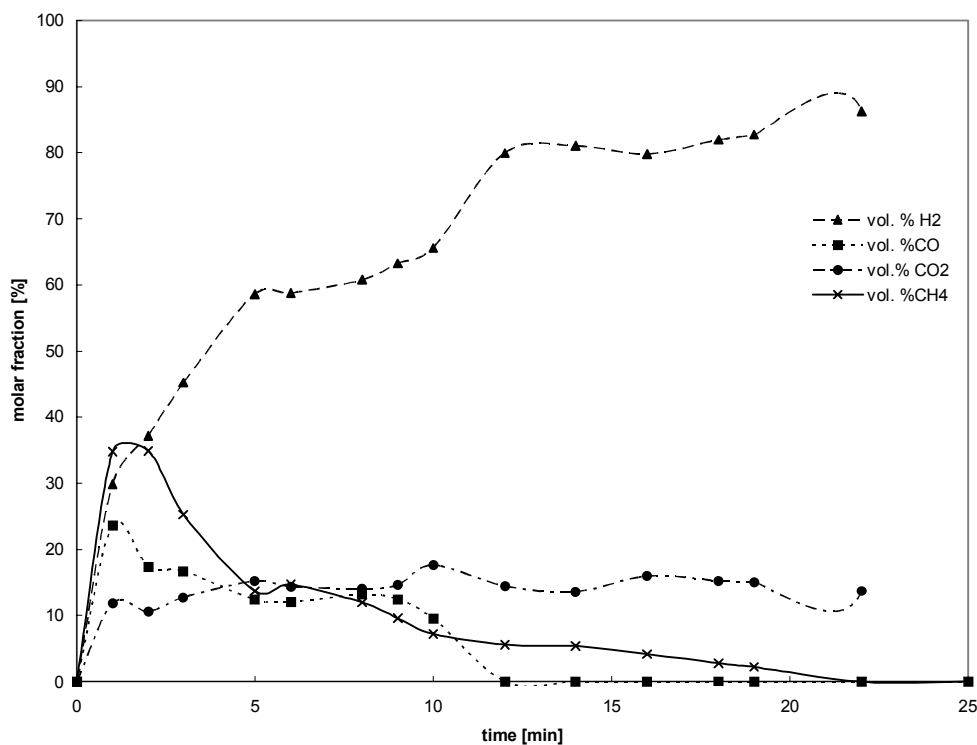


Figure 27 Typical product distribution as a function of time in a fluidized bed reactor

REFERENCES

1. Ageeva, T. V., Chernenkov, I. I., "Industrial Hydrogen Production by means of coal gasification" *Khimiya Tverdogo Topliva*, 6, 51-55 (1993)
2. Balasubramanian, B, Ortiz, A. L., Kaytakuglu, S., Harrison, D. P., "Hydrogen from methane in a single step process", *Chem. Eng. Sci.*, 54, 3543 -3552 (1999)
3. Brage, C., Qizhuang, Y., Sjostrom, K., "Characteristics of evolution of tar from wood pyrolysis in a fixed-bed reactor", *Fuel*, 75 (2), 213-219 (1996)
4. Cox, A. W., "Hydrogen from coal – Prospects and challenges", *Energy World*, 321, 10 (2004)
5. Curran, G. P., Clancey, J. T., Scarpillo, D. A., Fink, C. E., Gorin, E., "Carbon dioxide acceptor process", *Chemical Engineering Progress*, 62 (2), 80-86 (1966)
6. De Biasi, V., "FutureGn IGCC to convert coal into hydrogen and electric power" *Gas Turbine World*, 33 (4), 12 -14 +16 (2003)
7. Egan, B. Z., Fain, D. E., Roettger, G. E., White, D. E., "Separating hydrogen from coal gasification gases with alumina membranes", *ASME*, 5 (1991)
8. Egan, B. Z., Fain, D. E., Roettger, G. E., White, D. E., "Separating hydrogen from coal gasification gases with alumina membranes", *J. Engr. Gas Turbines and Power, Transactions of the ASME*, 114 (2), 367-370 (1992)
9. Garcia, X. A., Alarcon, N. A., Gordon, A. L., "Steam gasification of tars using a CaO catalyst". *Fuel Processing Technology*, 58 (2), 83-102 (1999)
10. Hauserman, W. B., "high Yield Hydrogen Production by Catalytic Gasification of Coal or Biomass", *Int J. of Hydrogen Energy*, 19(5), 413-419 (1994)
11. Hesp, W. R., Waters, P. L., "Thermal Cracking Of Tars And Volatile Matter From Coal Carbonization", *Ind Eng Chem Prod Res Develop*, 9 (2), 194-202 (1970)
12. Hilaire, S., Wang, X., Luo, T., Gorte, R. J., Wagner, J., "A comparative study of the water gas shift reaction over ceria supported metallic catalysts" *Applied Catalysis A: General*, 215 (1-2), 271-278 (2001).
13. I. J. Moon, C. H. Rhee, "Reduction behavior of hematite compacts by H₂ and H₂-CO gas mixtures", *Proc of the 1997 TMS Annual Meeting*, Feb 9-13, Orlando, FL, Minerals Metals and Materials Society, Warrendale, PA, USA, (1997) 649.
14. I. J. Moon, C. H. Rhee, D. J. Min, "Reduction behavior of hematite compacts by H₂-CO gas mixtures" *Steel Research*, 69 (1998) 302
15. K. Ishii, T. Akiyama, Y. Kashiwaya, S. Kondo, *Memoirs of the Faculty of Engineering*, Hokkaido University, Sapporo, Japan, 17 (1986) 1
16. Kuramoto, K., Furuya, T., Suzuki, Y., hatano, H., Kumabe, K., Yoshiie, R., Moritomi, H., Shi-Ying, L, "Coal gasification with a subcritical steam in the presence of a CO₂ sorbent: Products and conversion under transient heating", *Fuel Processing Technology*, 82 (1), 61-73 (2003)
17. Li, Y.X, Song, J.; Li, C.H.; Guo, H.X.; Xie, K.C., "A study of high temperature desulfurization and regeneration using iron-calcium oxides in a fixed-bed Reactor", *J. of Chem Engr of Chinese Univ.*, 15(2), 133 – 137 (2001).

18. Lin, S., Harada, M., Suzuki, Y., Hatano, H., "Continuous Experiment regarding Hydrogen Production by Coal/CaO reaction with Steam (I) Gas Products", *Fuel*, 83 (7-8), 869-874 (2004)
19. Lin, S., Harada, M., Suzuki, Y., Hatano, H., "Hydrogen production from coal by separating carbon Dioxide during Gasification", *Fuel*, 81 (16), 2079-2085 (2002)
20. Lin, S., Suzuki, Y., Hatano, H., Oya, M., Harada, M., "Innovative Hydrogen Production by Reaction Integrated Novel Gasification Process (HyPr-RING)", *J. South African Inst. Of Mining And Metall.*, 101 (1), 53 – 59 (2001)
21. M. J. Tiernan, P. A. Barnes, G. M. B. Parkes, "Reduction of iron oxide catalysts: the investigation of kinetic parameters using rate perturbation and linear heating thermoanalytical techniques", *J. Phys Chem. B*, 105 (2001) 220
22. M. Shimokawabe, *Thermochim. Acta.*, 28 (1979) 287
23. M. V. C. Sastri, R. P. Viswanath; B. Viswanath, "Studies on the reduction of iron with hydrogen", *Int. J. Hydrogen Energy*, 7 (1982) 951
24. McCoy, D. C., Curran, G. P., Sudbury, J. D., "CO₂ Acceptor Process Pilot Plant 1976", *Automotive Industries*, 33-51 (1976)
25. Minowa, T., Inoue, S., "Hydrogen production from biomass by catalytic gasification in hot compressed water", *Renewable Energy*, 16 (1-4 pt 2), 1114-1117 (1999)
26. Nikanorova, L. P., Antonova, V. M., „Combiend Reduction of Iron Oxide Coantact by Lignite and Gas in the Process of Hydrogen Production” *Khimiya Tverdogo Topliva*, 4, 138 – 142 (1991)
27. Ohtsuka, Y., Tomita, A., "Calcium Catalysed Steam Gasification Of Yallourn Brown Coal", *Fuel*, 65 (12), 1653-1657 (1986)
28. Otsuka, K., Mito, A., Takenaka, S., Yamanaka, I., "Production of hydrogen from methane without CO₂-emission mediated by indium oxide and iron oxide", *Int. J. Hyd. Energy.*, 26 (3) 191-194 (2001)
29. Pierce, J., "Gasification of coal could provide clean energy", *Engineer*, 292 (7692), 10 (2003)
30. Prilepskaya, L.L.; Iskhakov, Kh.A., "Thermal destruction of coal with additions of iron oxides", *Khimiya Tverdogo Topliva*, 4, 62 – 65 (1991).
31. Qi, X., Flytzani – Stephanopoulos, M., "Activity and Stability if Cu-CeO₂ catalysts in high Temepreature water-gas shift for fuel cell applications", *Ind. Eng. Chem. Res.*, 43 (12), 3055 – 3062(2004)
32. Ruby, J., Johnson, A. A., Ziocck, H., "Gasification for carbon capture and zero emission", *2004 SME Annual Meeting Preprints, 2004 SME Annual Meeting Preprints*, 961-968 (2004)
33. Rukowski, M. D., DeLallo, M. R., Klett, M. G., Badin, J. S., Temchin, J. R., „Coal Processing plants for hydrogen production with CO₂ Capture”, *Technology: Journal of the Franklin Institute*, 8 (4-6), 149-158 (2002).
34. Vamvuka, D., "Gasification of Coal", *Energy Exploration and Exploitation*, 17 (6), 515-582 (1999)
35. Wang, J., Takarada, T., "Role of calcium hydroxide in supercritical water gasification of low-rank coal", *Energy and Fuels*, 15 (2), 356-362 (2001)

36. Zhao, S., Gorte, R. J., "The activity of Fe-Pd for the water gas shift reaction", *Cat. Lett.*, 92 (1-2), 75 -80 (2004).
37. Zhu, T – Y., Wang, Y., "Effect of Fe₂O₃ - K₂CO₃ on coal mild gasification", *Chemical Reaction Engineering and Technology*, 16 (2), 203 – 208 (2000).